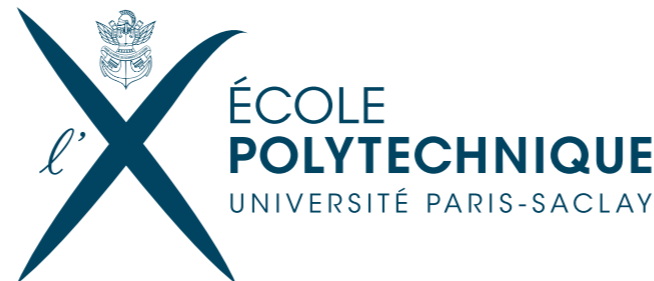
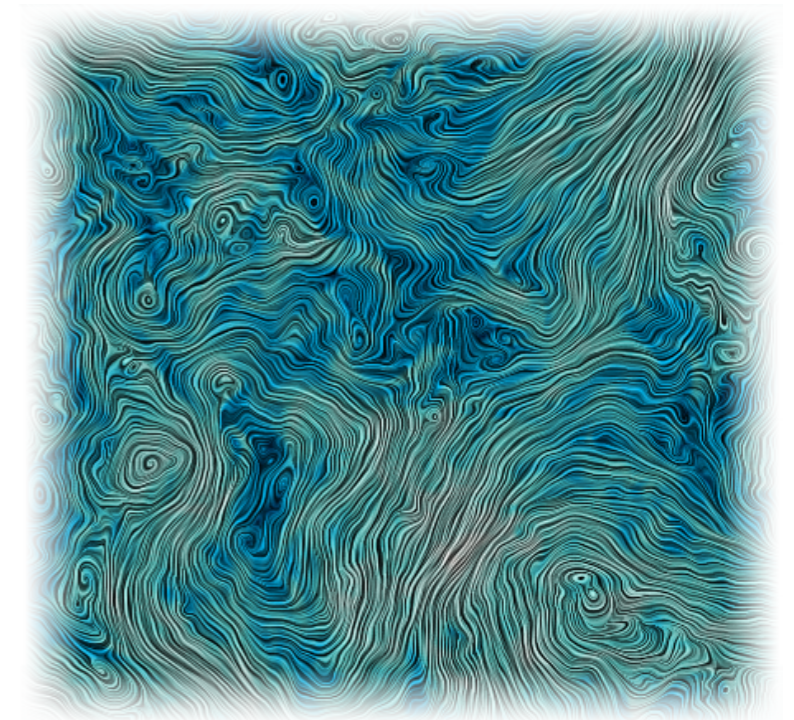


Gauging anisotropic scaling in plasma turbulence and topological change at the ion scales

Khurom H. Kiyani

Romain Meyrand, Fouad Sahraoui, Sandra Chapman



Theme issue on the topic of plasma turbulence

**PHILOSOPHICAL
TRANSACTIONS A**

Volume 373 | Issue 2041 | 13 May 2015

Contents

Theme issue: Dissipation and heating in solar wind turbulence

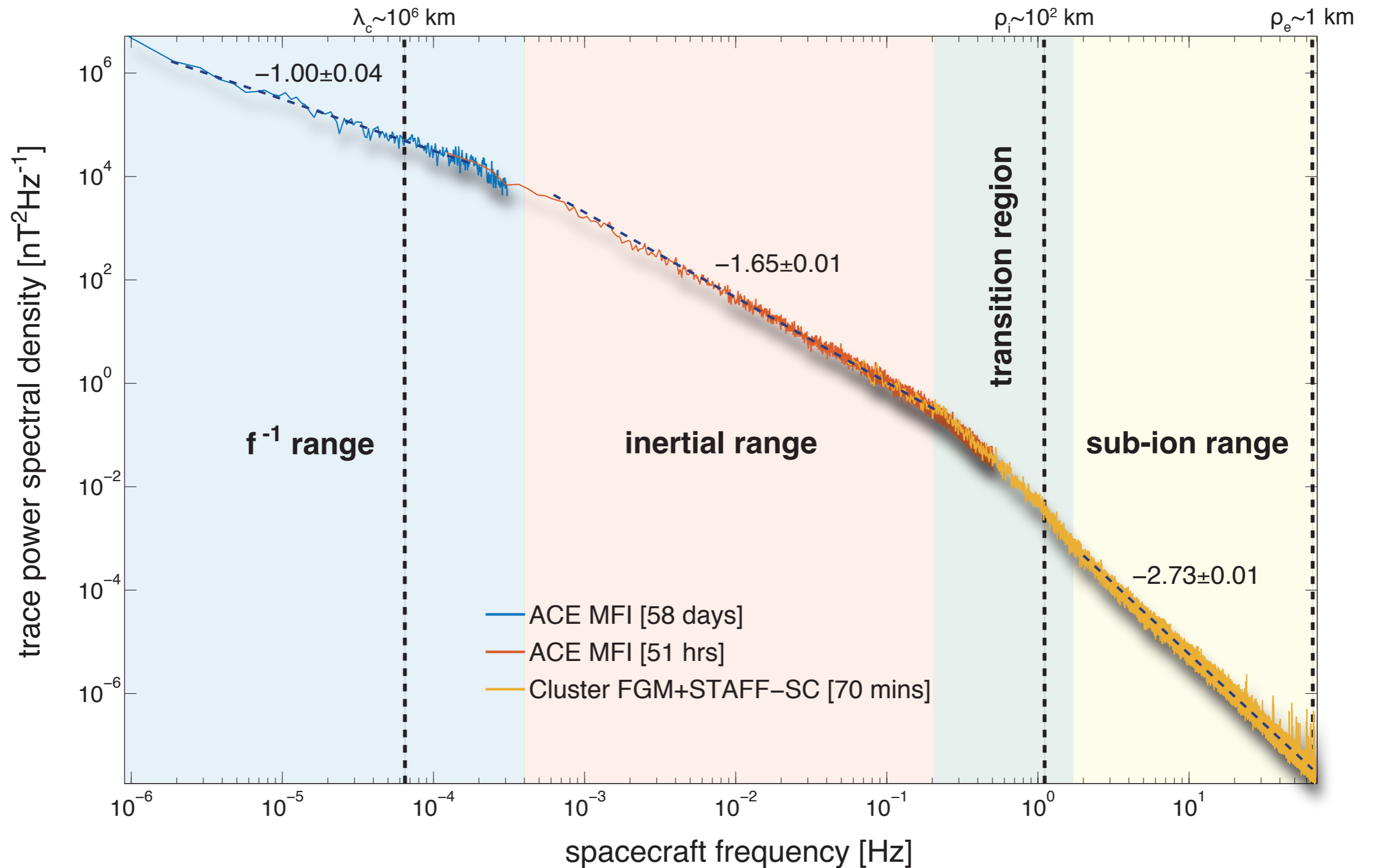
	Article ID		Article ID
INTRODUCTION			
Dissipation and heating in solar wind turbulence: from the macro to the micro and back again KH Kiyani, KT Osman and SC Chapman	20140155	Short-wavelength plasma turbulence and temperature anisotropy instabilities: recent computational progress SP Gary	20140149
ARTICLES			
Intermittency, nonlinear dynamics and dissipation in the solar wind and astrophysical plasmas WH Matthaeus, M Wan, S Servidio, A Greco, KT Osman, S Oughton and P Dmitruk	20140154	A dynamical model of plasma turbulence in the solar wind GG Howes	20140145
The role of turbulence in coronal heating and solar wind expansion SR Cranmer, M Asgari-Targhi, MP Miralles, JC Raymond, L Strachan, H Tian and LN Woolsey	20140148	Kinetic scale turbulence and dissipation in the solar wind: key observational results and future outlook ML Goldstein, RT Wicks, S Perri and F Sahraoui	20140147
Third-moment descriptions of the interplanetary turbulent cascade, intermittency and back transfer JT Coburn, MA Forman, CW Smith, BJ Vasquez and JE Stawarz	20140150	Dynamic properties of small-scale solar wind plasma fluctuations MO Riazantseva, VP Budaev, LM Zelenyi, GN Zastenker, GP Pavlos, J Safrankova, Z Nemecek, L Prech and F Nemec	20140146
Anisotropy in solar wind plasma turbulence S Oughton, WH Matthaeus, M Wan and KT Osman	20140152	Generation of magnetic holes in fully kinetic simulations of collisionless turbulence V Roytershteyn, H Karimabadi and A Roberts	20140151
		Turbulent reconnection and its implications A Lazarian, G Eyink, E Vishniac and G Kowal	20140144

Theme issue on the topic of plasma turbulence

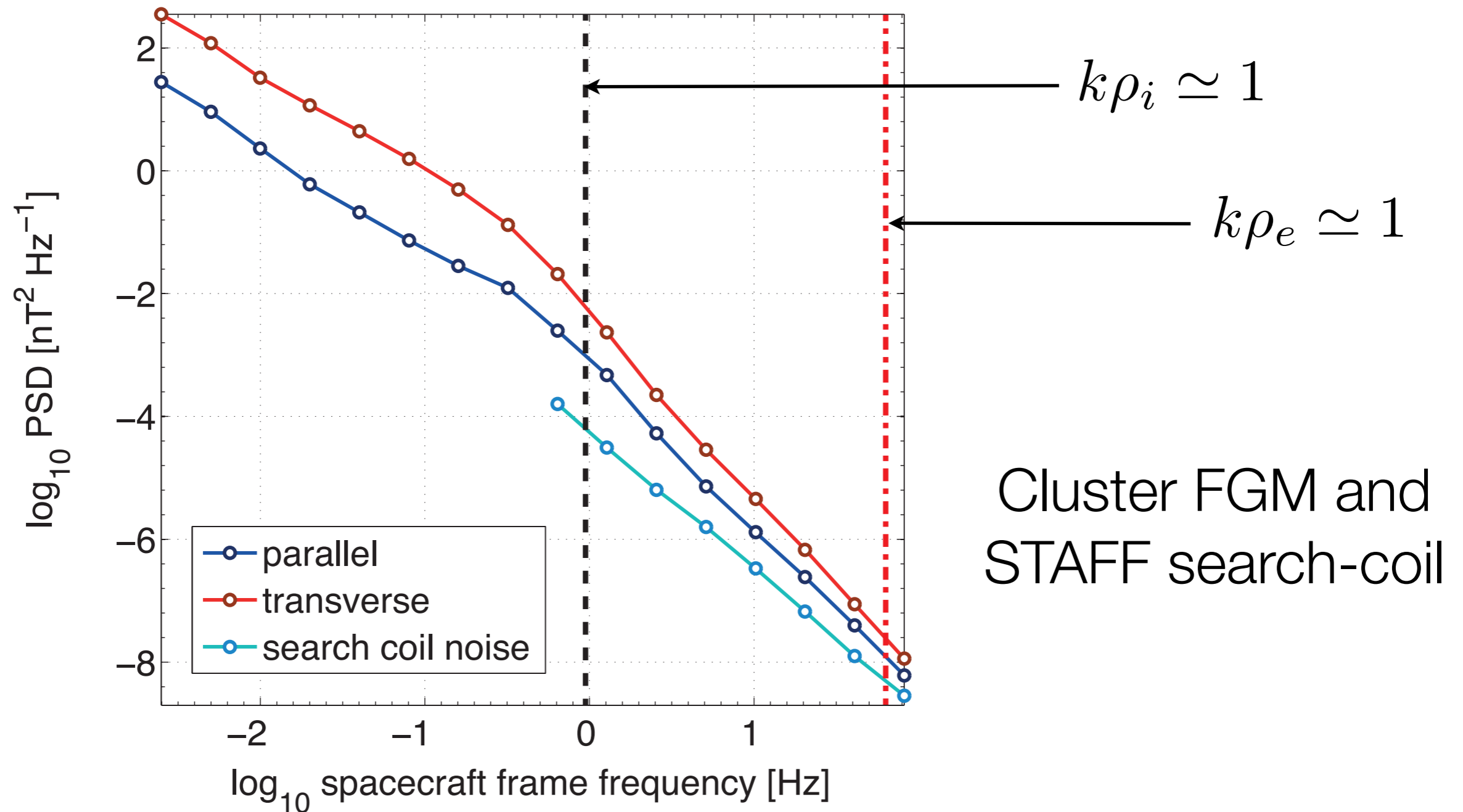


[http://
www.warwick.ac.uk/fac/
sci/physics/research/
cfsa/people/kiyani/
philstransa.zip](http://www.warwick.ac.uk/fac/sci/physics/research/cfsa/people/kiyani/philstransa.zip)

Typical spectral density of solar wind turbulence

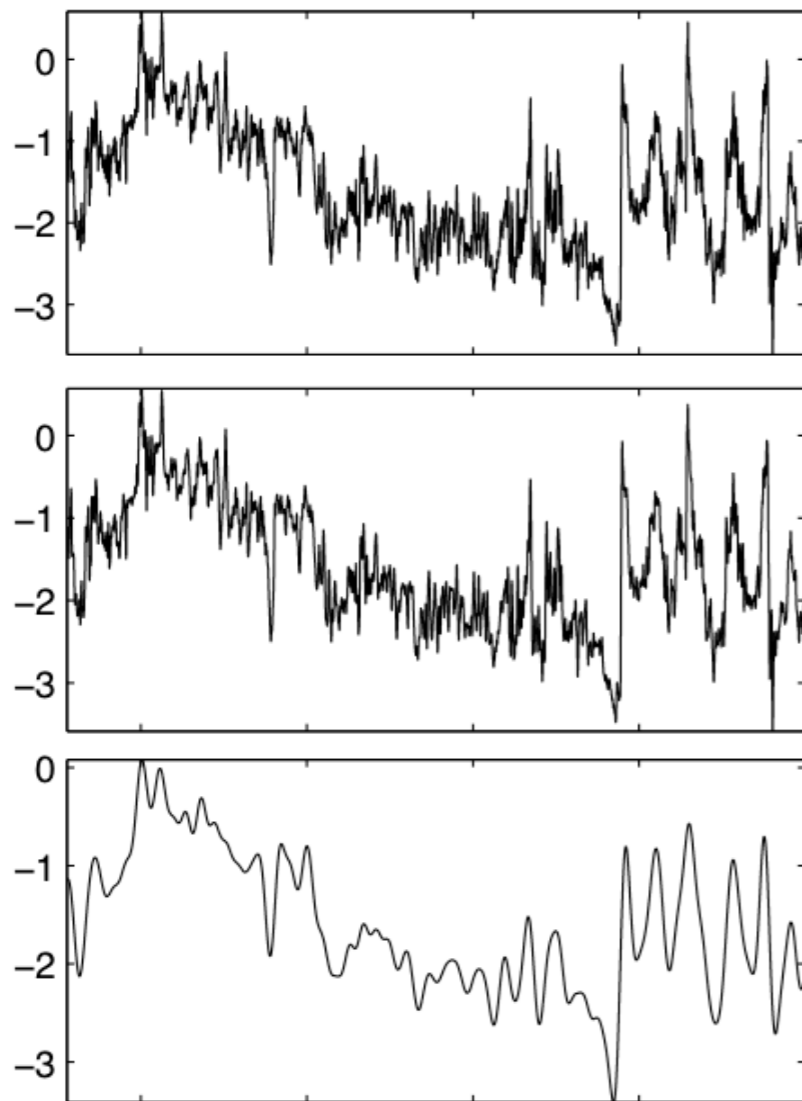


power spectral density {component anisotropy}

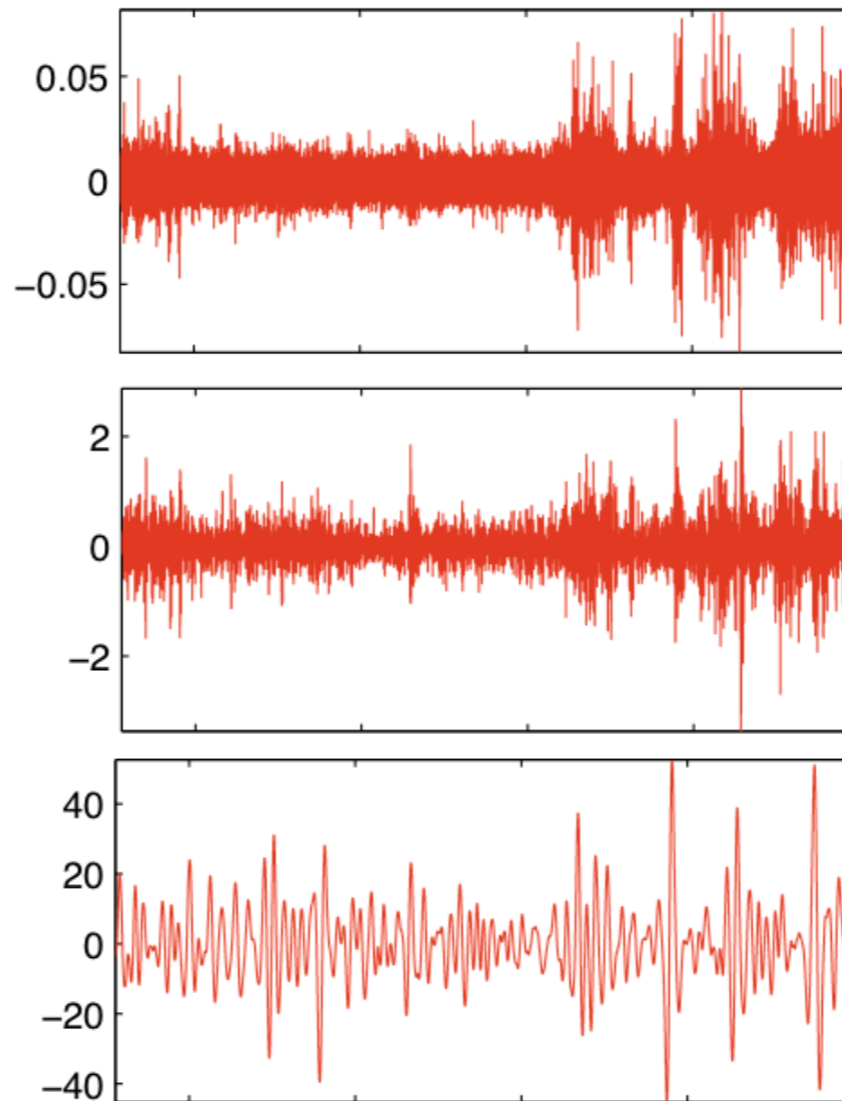


adaptive local scale-dependent fluctuations **and** background guide field

background field



fluctuations

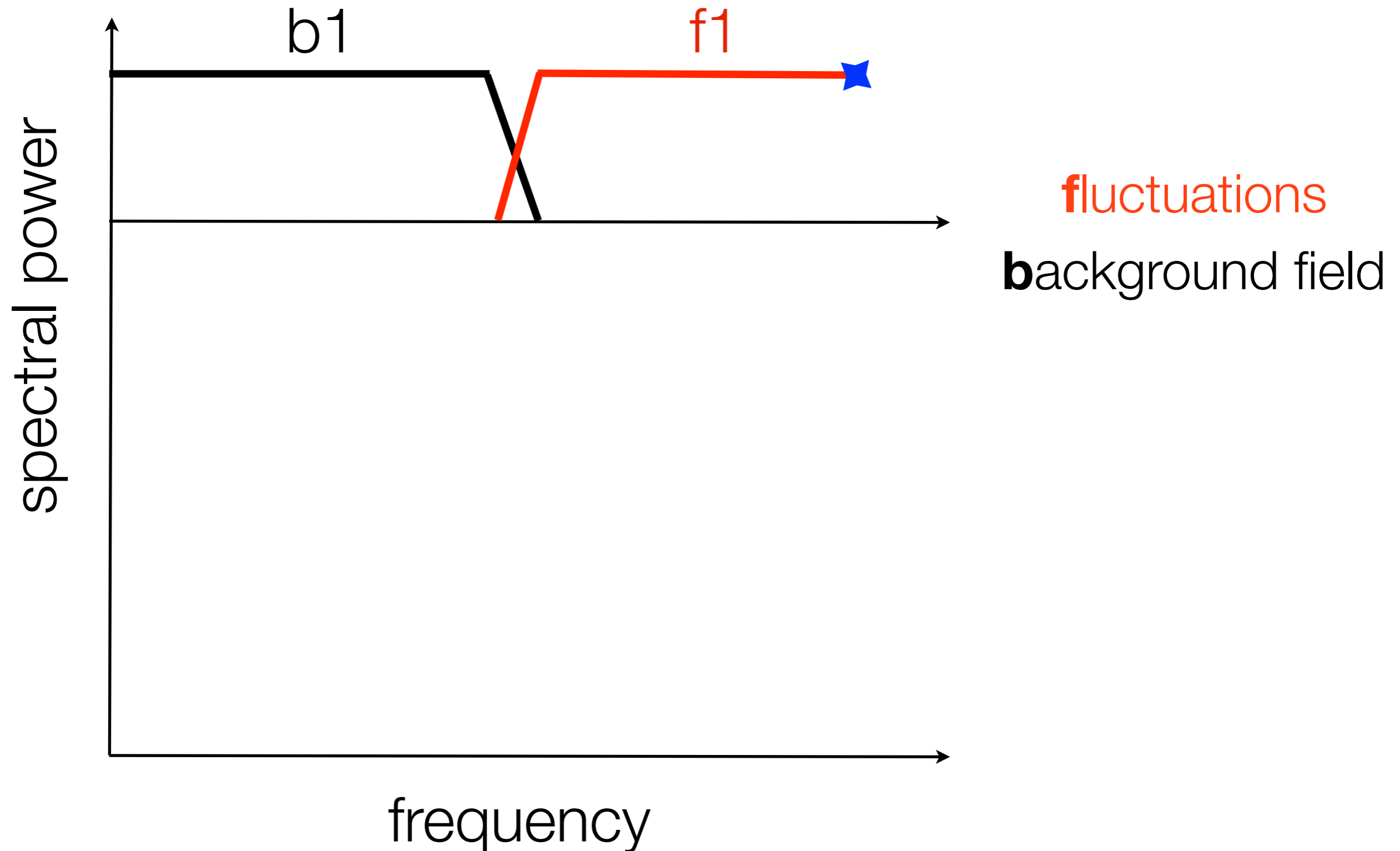


small
scales

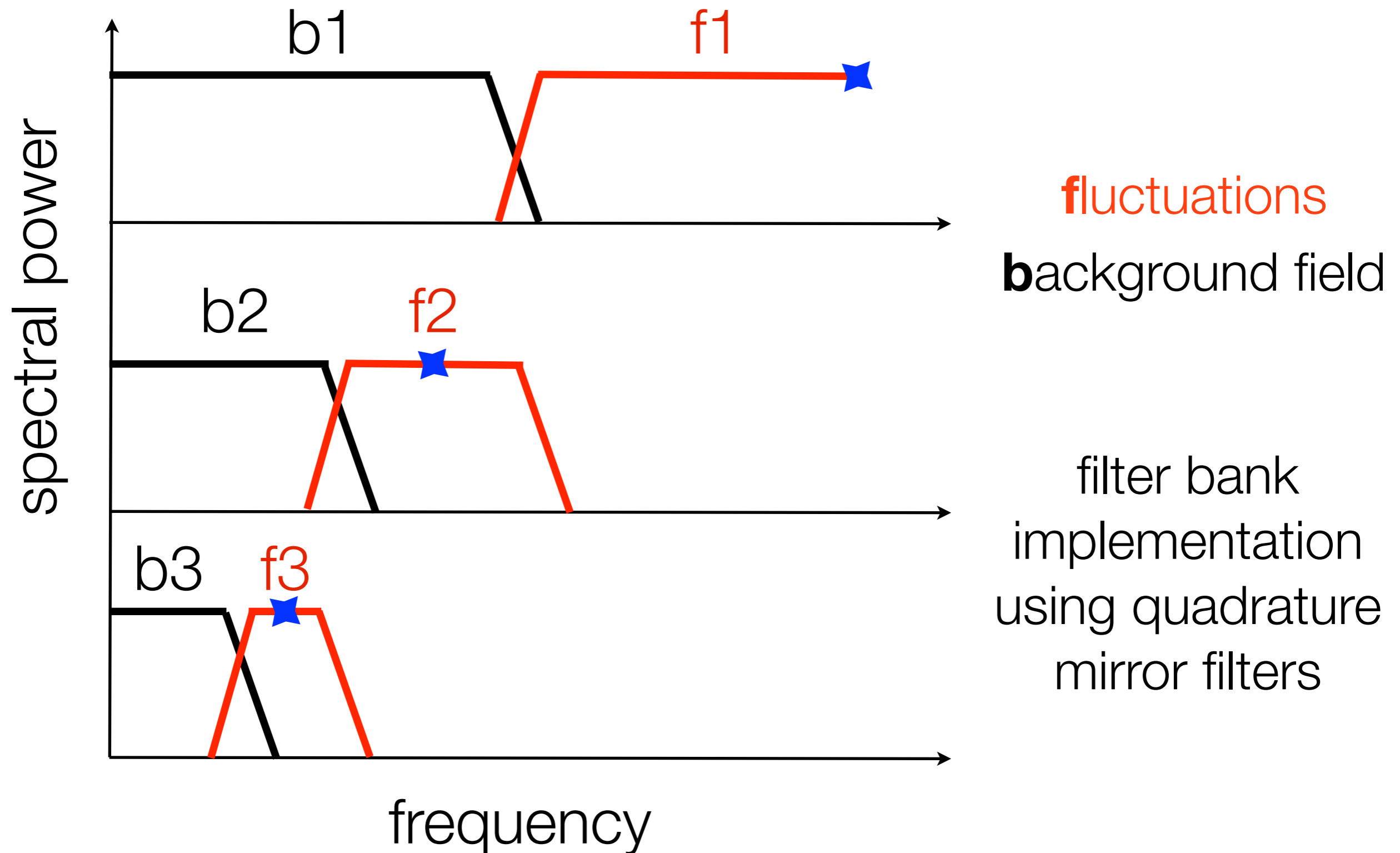
large
scales



local scale-dependent fluctuations *and* background field using low/high pass filters

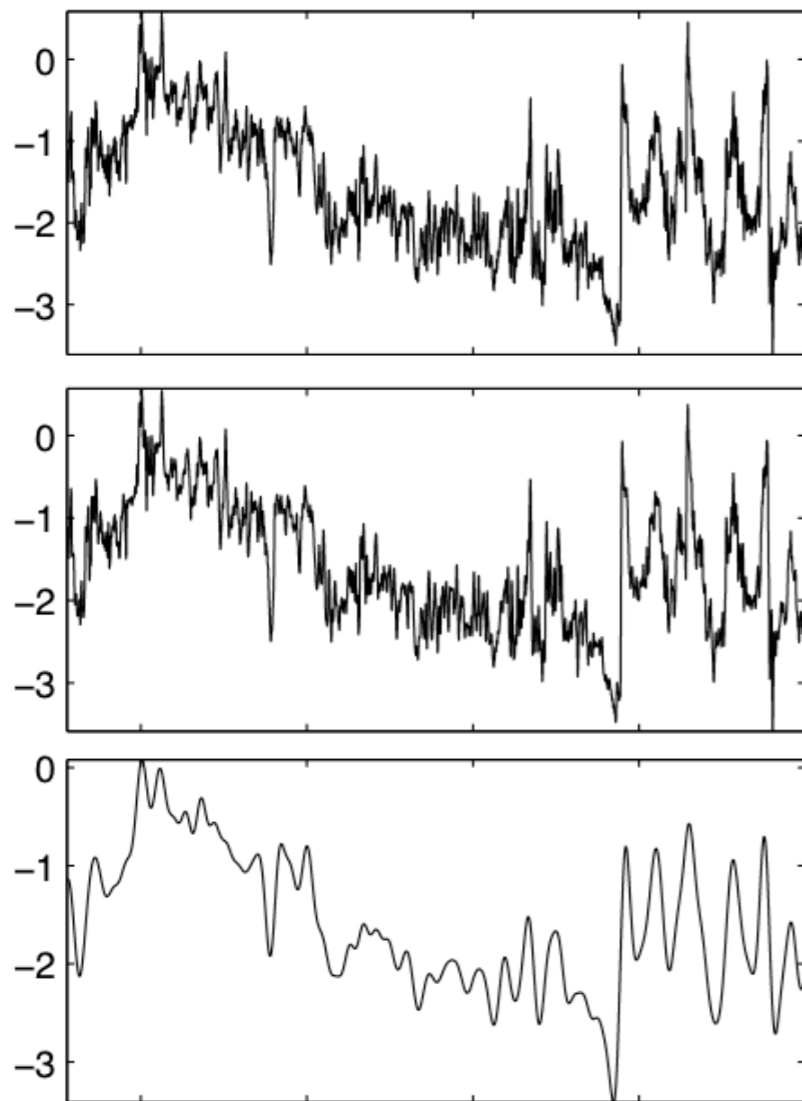


local scale-dependent fluctuations *and* background field using low/high pass filters

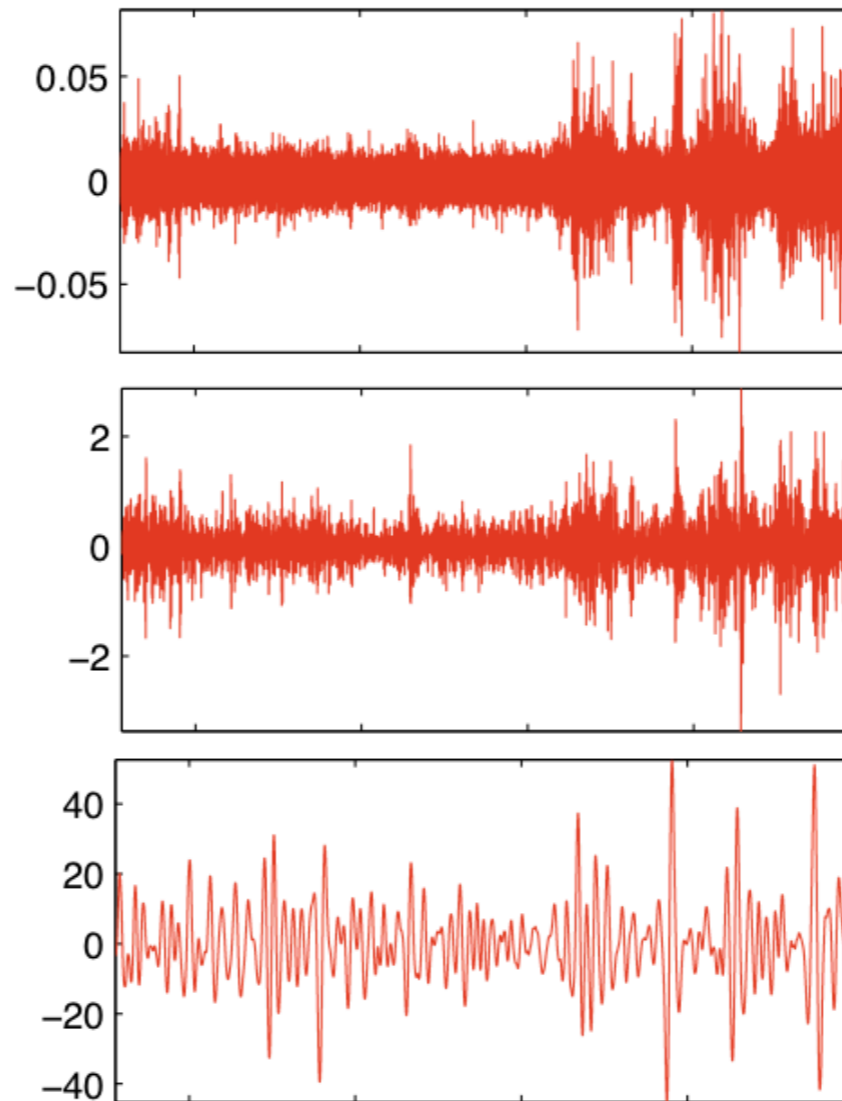


adaptive local scale-dependent fluctuations **and** background guide field

background field



fluctuations



small
scales

large
scales

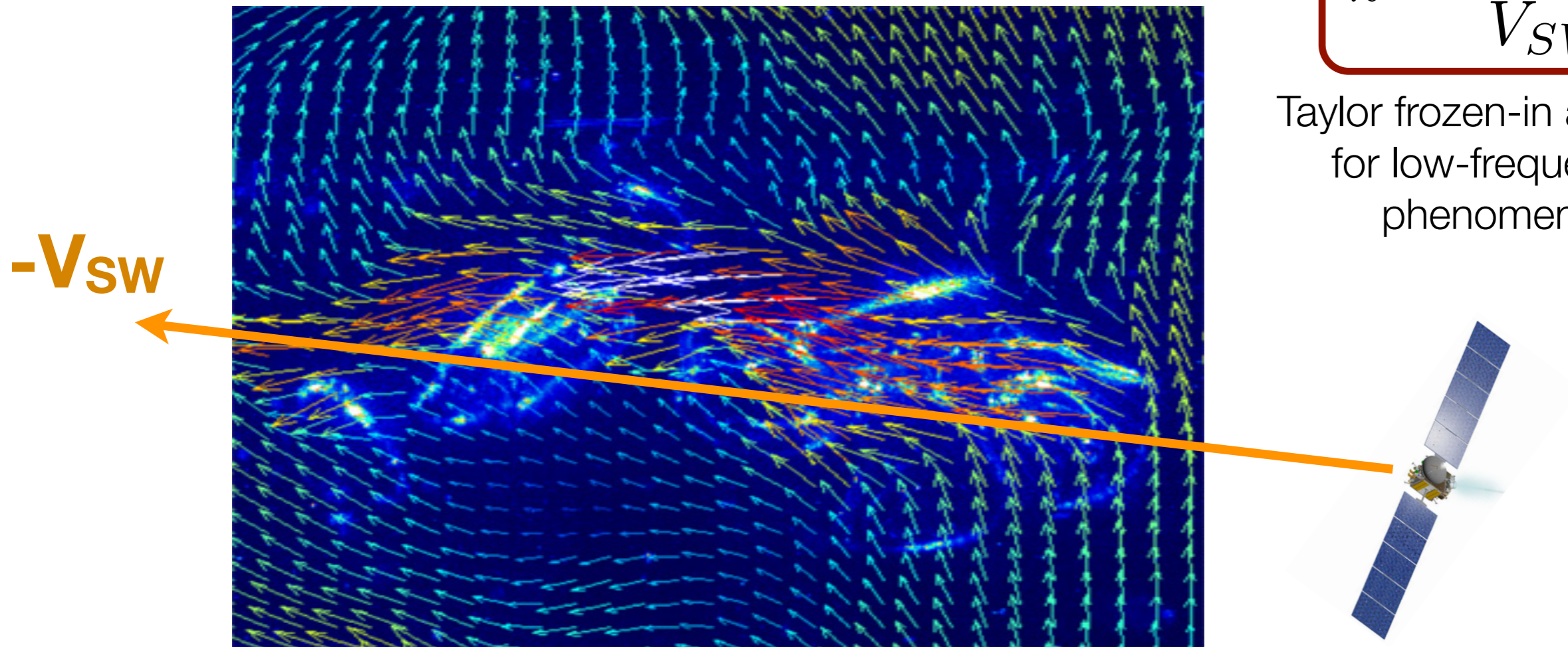


Each band (fluctuations) has its corresponding background field

angles of measurement w.r.t. B

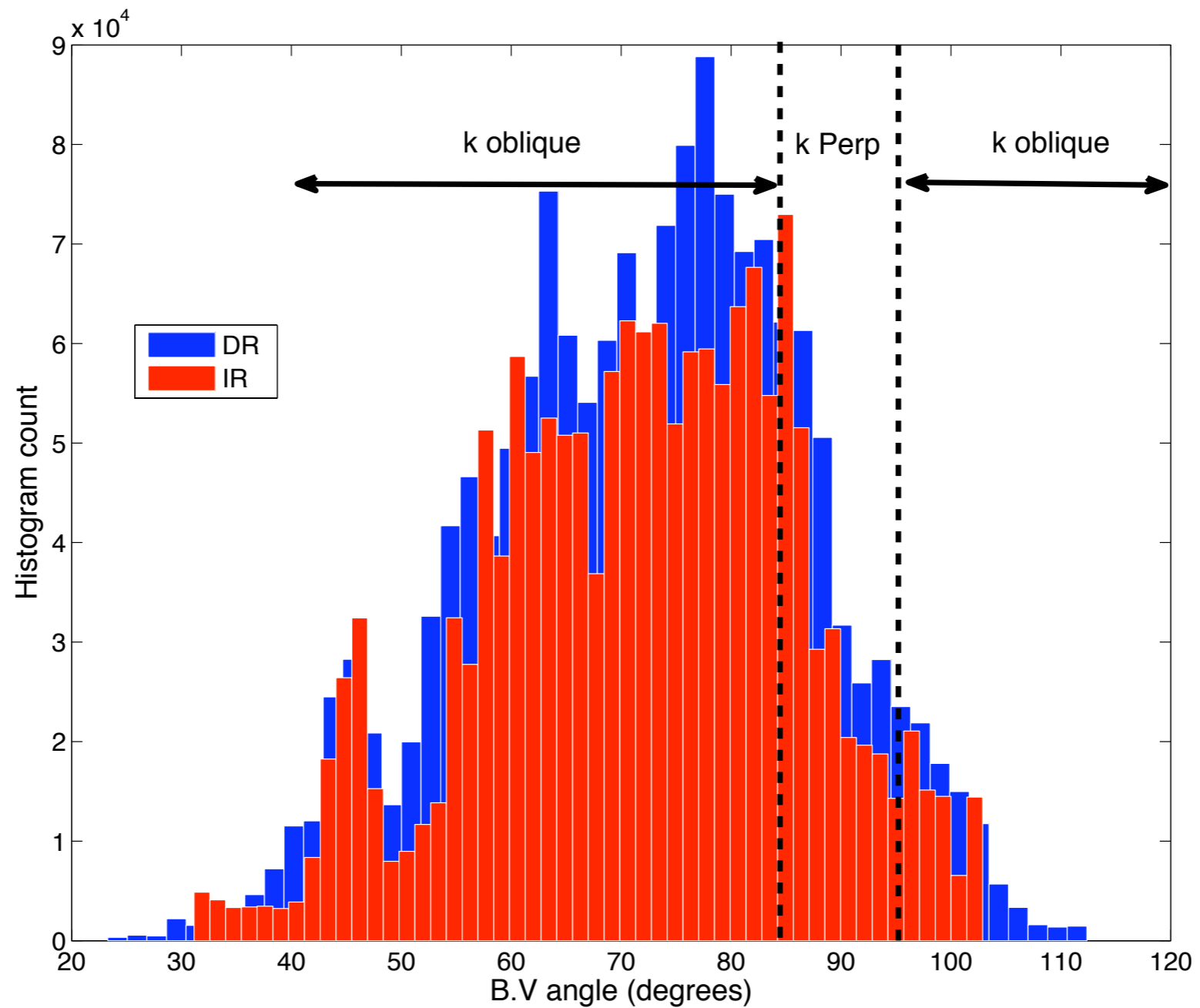
$$k = \frac{2\pi f_{sc}}{V_{SW}}$$

Taylor frozen-in approx,
for low-frequency
phenomena



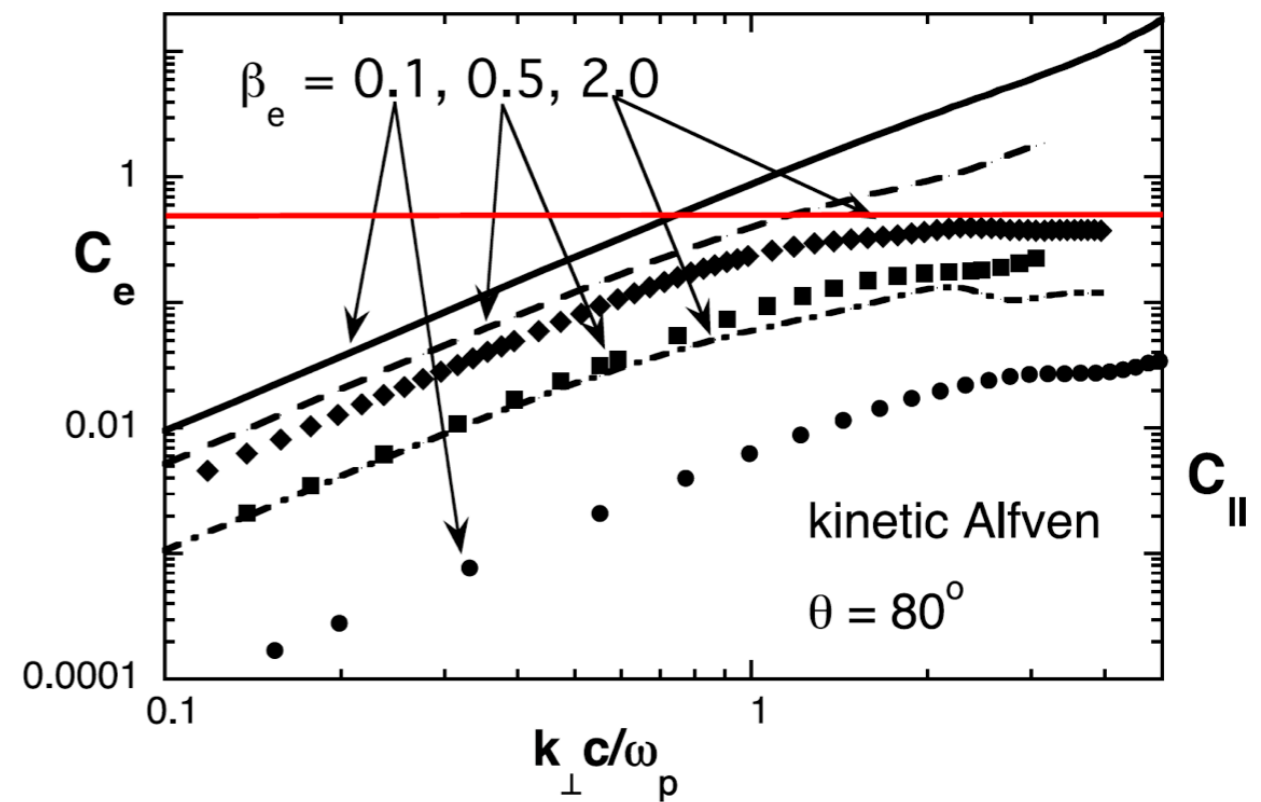
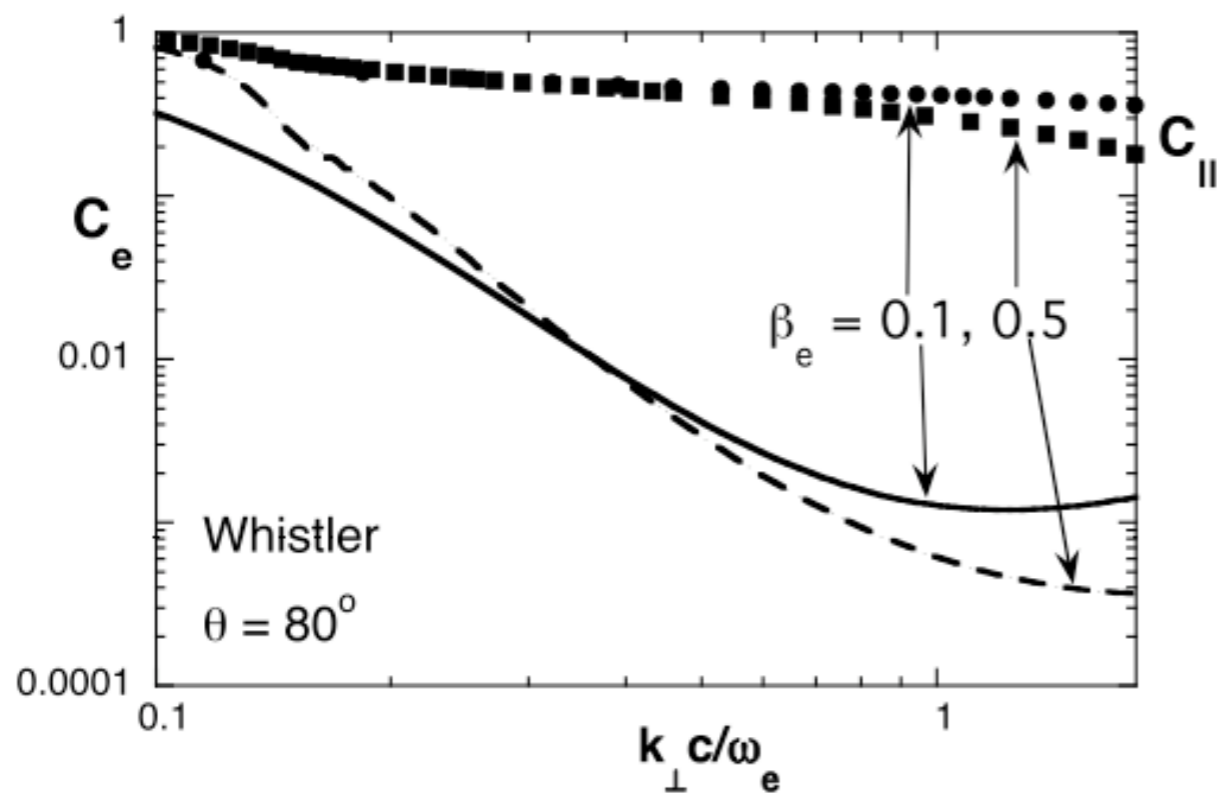
$$\text{MHD } \frac{V_A}{V_{SW}} < 1 \quad \text{else} \quad \frac{V_\phi}{V_{SW}} < 1$$

Anisotropy (angle between B and V)



Magnetic Compressibility and linear wave modes

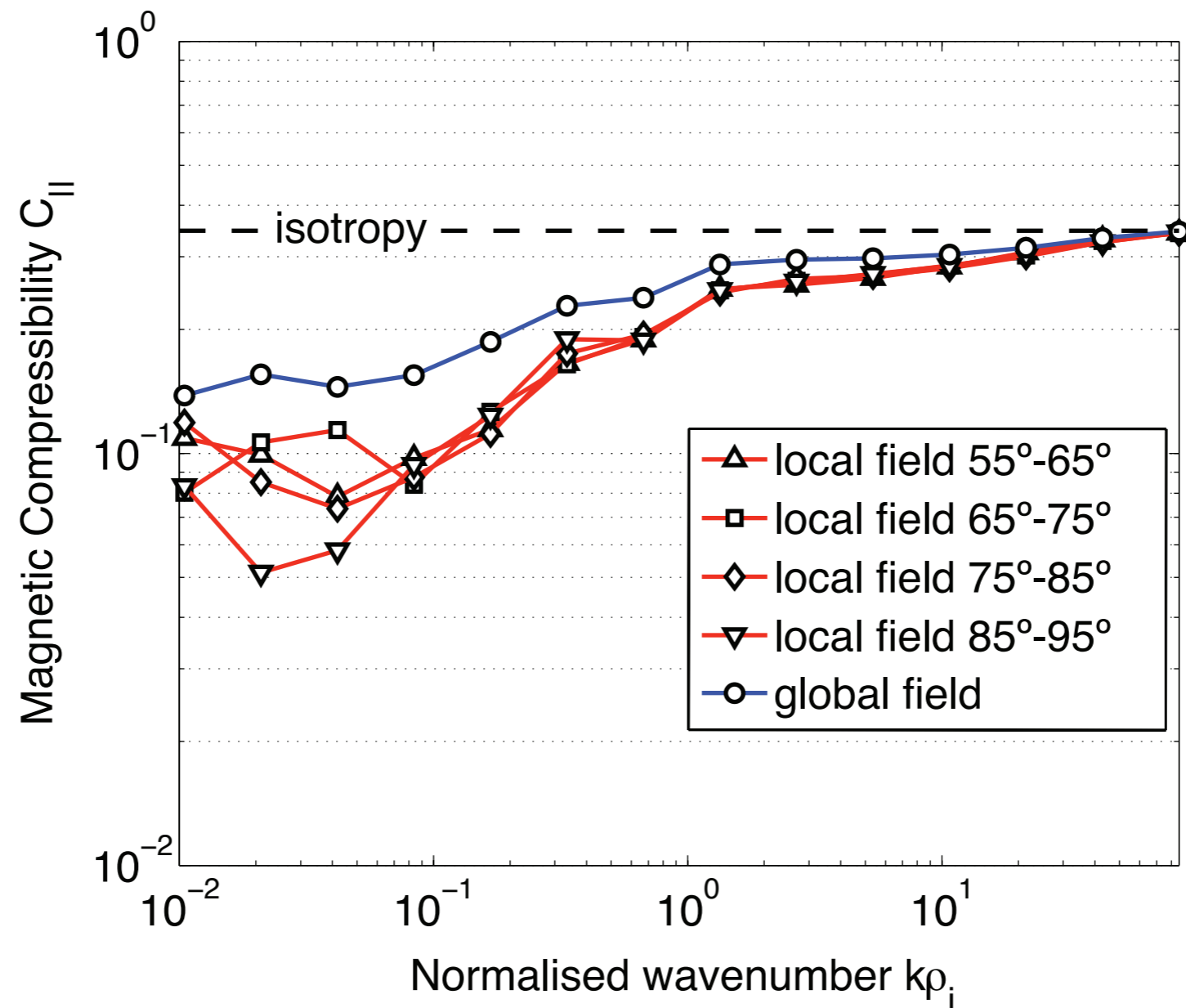
$$C_{\parallel}(\mathbf{k}) \equiv \frac{|\delta B_{\parallel}(\mathbf{k})|^2}{|\delta \mathbf{B}(\mathbf{k})|^2}.$$



S P. Gary and C. W. Smith,
J. Geophys. Res **114**, A12105 (2009).

magnetic compressibility

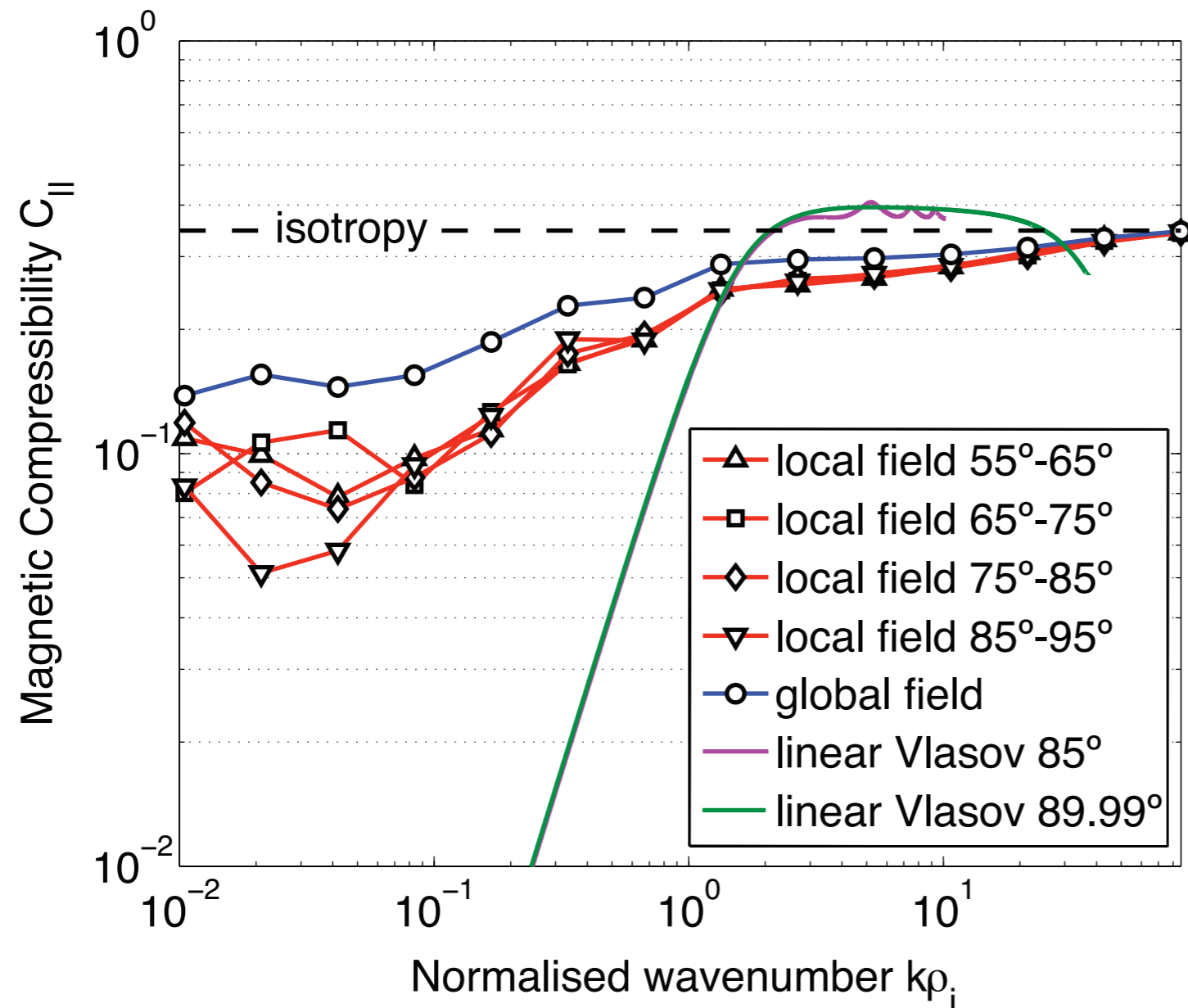
$$C_{\parallel}(f) = \frac{1}{N} \sum_{j=1}^N \frac{\delta B_{\parallel}^2(t_j, f)}{\delta B_{\parallel}^2(t_j, f) + \delta B_{\perp}^2(t_j, f)}$$



Kiyani et al.
ApJ (2013)

kinetic Alfvén wave fluctuations

$$C_{\parallel}(f) = \frac{1}{N} \sum_{j=1}^N \frac{\delta B_{\parallel}^2(t_j, f)}{\delta B_{\parallel}^2(t_j, f) + \delta B_{\perp}^2(t_j, f)}$$



Kiyani et al.
ApJ (2013)

Gary & Smith (2009)

Salem et al. (2012)
TenBarge et al. (2012)

Hall physics

Hall-MHD model

$$\frac{\partial \mathbf{B}}{\partial t} = \nabla \times (\mathbf{v} \times \mathbf{B}) + \frac{1}{\mu e n_e} \nabla \times (\mathbf{B} \cdot \nabla \mathbf{B}) + \eta \nabla^2 \mathbf{B}$$

inertial range

$$k\rho_i \ll 1$$

convective term
dominates

[B-field frozen to ions]

dissipation range

$$k\rho_i > 1$$

Hall term dominates
[ions demagnetise]

Hall physics

$$\frac{\partial \mathbf{B}}{\partial t} = \nabla \times (\mathbf{v} \times \mathbf{B}) + \frac{1}{\mu e n_e} \nabla \times (\mathbf{B} \cdot \nabla \mathbf{B}) + \eta \nabla^2 \mathbf{B}$$

assume in the inertial range

$$\nabla_{\perp} \gg \nabla_{\parallel} \quad [k_{\perp} \gg k_{\parallel}]$$

and

$$\delta B_{\perp} \gg \delta B_{\parallel}$$

supported by observations, simulations and theory

Hall physics

$$\frac{\partial \mathbf{B}}{\partial t} = \nabla \times (\mathbf{v} \times \mathbf{B}) + \frac{1}{\mu e n_e} \nabla \times (\mathbf{B} \cdot \nabla \mathbf{B}) + \eta \nabla^2 \mathbf{B}$$

$$\left. \frac{\partial \mathbf{B}_{\parallel}}{\partial t} \right|_{Hall} \sim \nabla_{\perp 1} \times (\mathbf{B} \cdot \nabla \delta \mathbf{B}_{\perp 2}) + \nabla_{\perp 2} \times (\mathbf{B} \cdot \nabla \delta \mathbf{B}_{\perp 1})$$

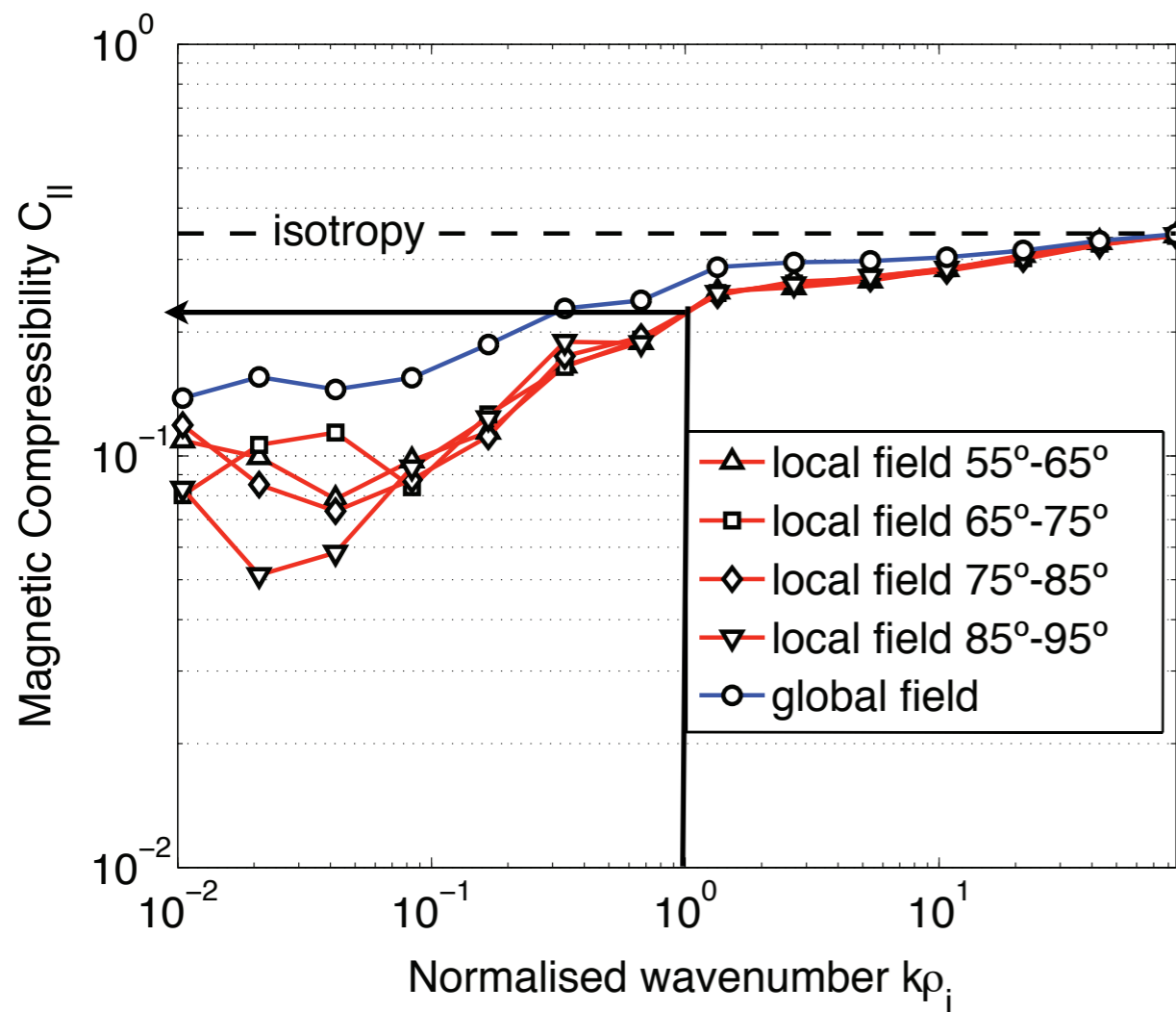
Hall physics

$$\frac{\partial \mathbf{B}}{\partial t} = \nabla \times (\mathbf{v} \times \mathbf{B}) + \frac{1}{\mu e n_e} \nabla \times (\mathbf{B} \cdot \nabla \mathbf{B}) + \eta \nabla^2 \mathbf{B}$$

$$\left. \frac{\partial \mathbf{B}_{\parallel}}{\partial t} \right|_{Hall} \sim \nabla_{\perp 1} \times (\mathbf{B} \cdot \nabla \delta \mathbf{B}_{\perp 2}) + \nabla_{\perp 2} \times (\mathbf{B} \cdot \nabla \delta \mathbf{B}_{\perp 1})$$

The Hall term **isotropises** components.

transition range



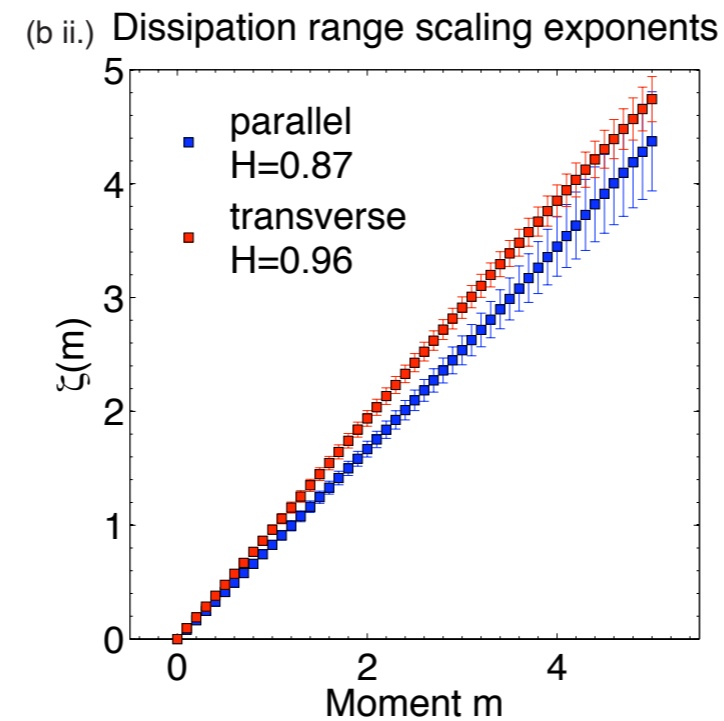
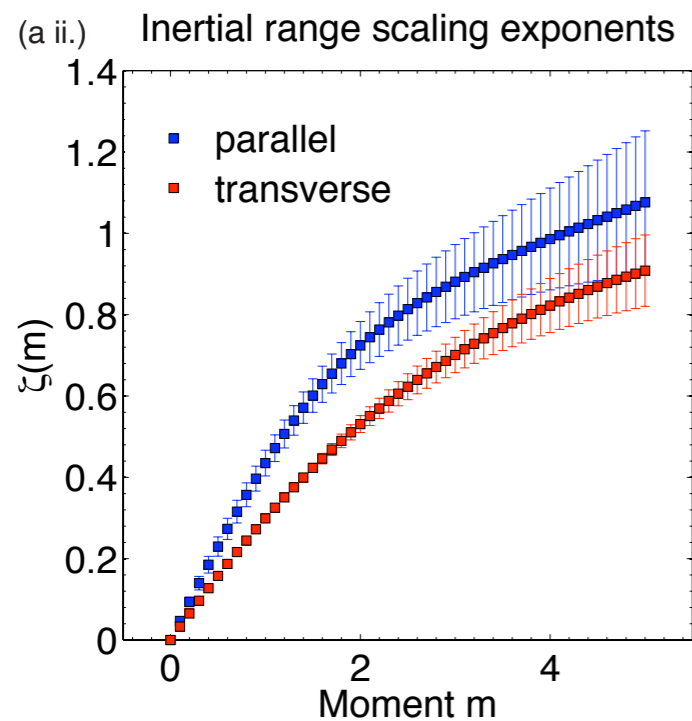
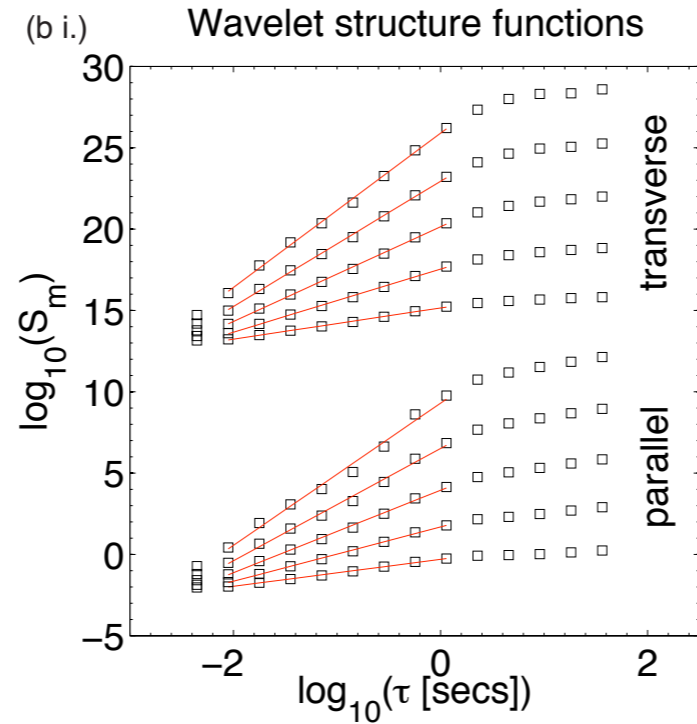
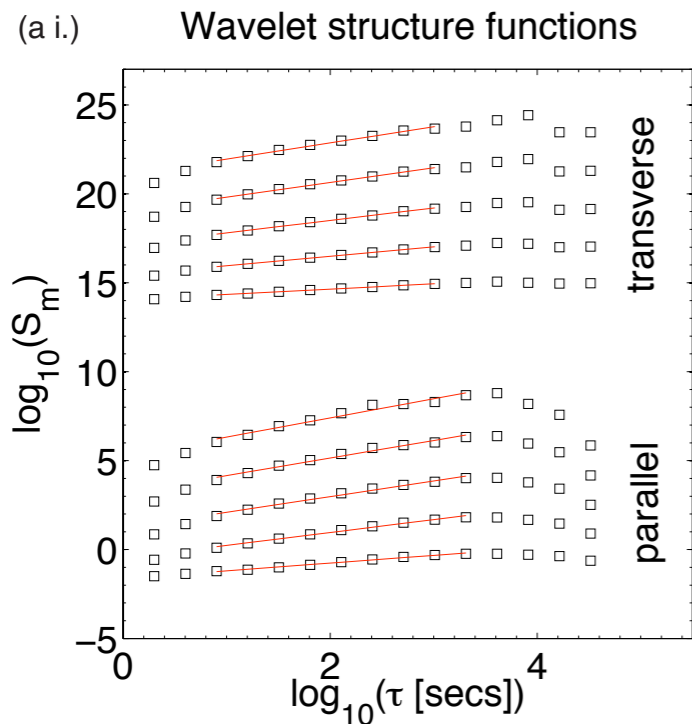
at $k\rho_i = 1$

Convective 50%

Hall 50%

$$C_{||} \simeq 0.5 \times 0.33 + 0.5 \times 0.1 \simeq 0.22$$

higher order scaling



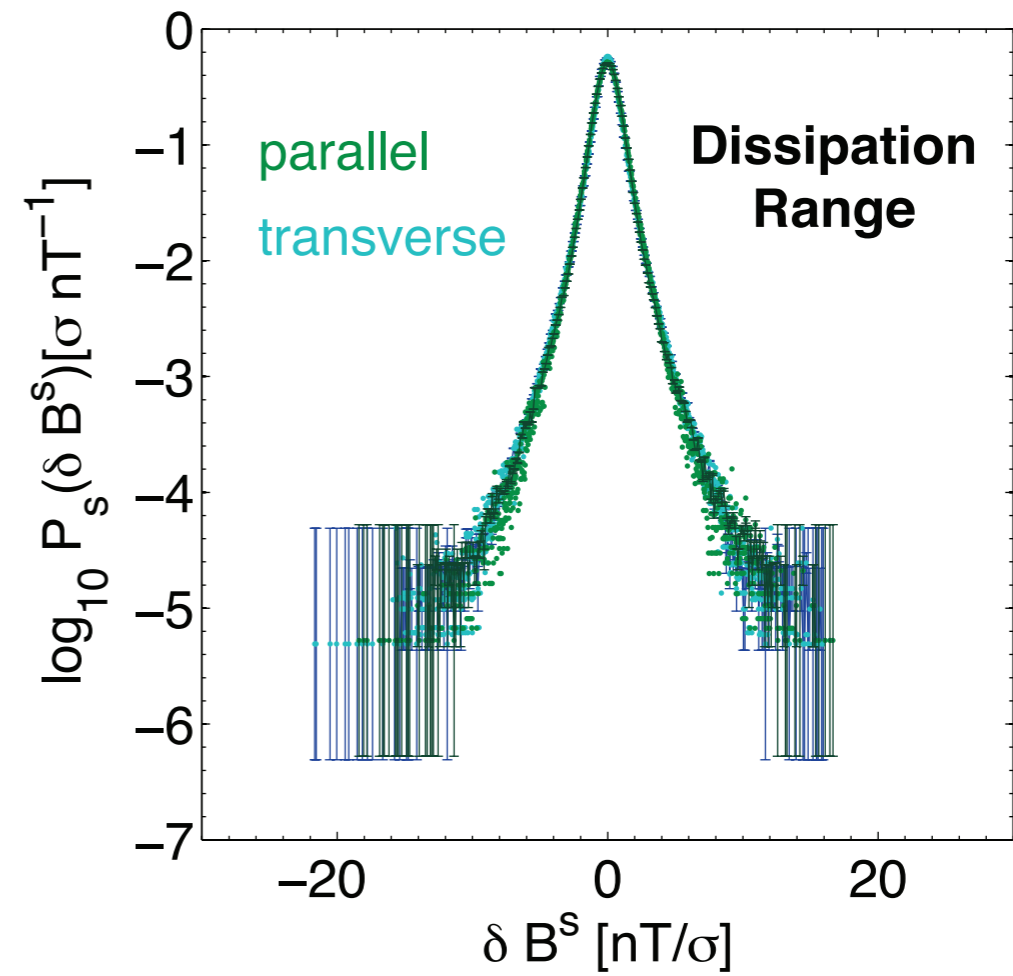
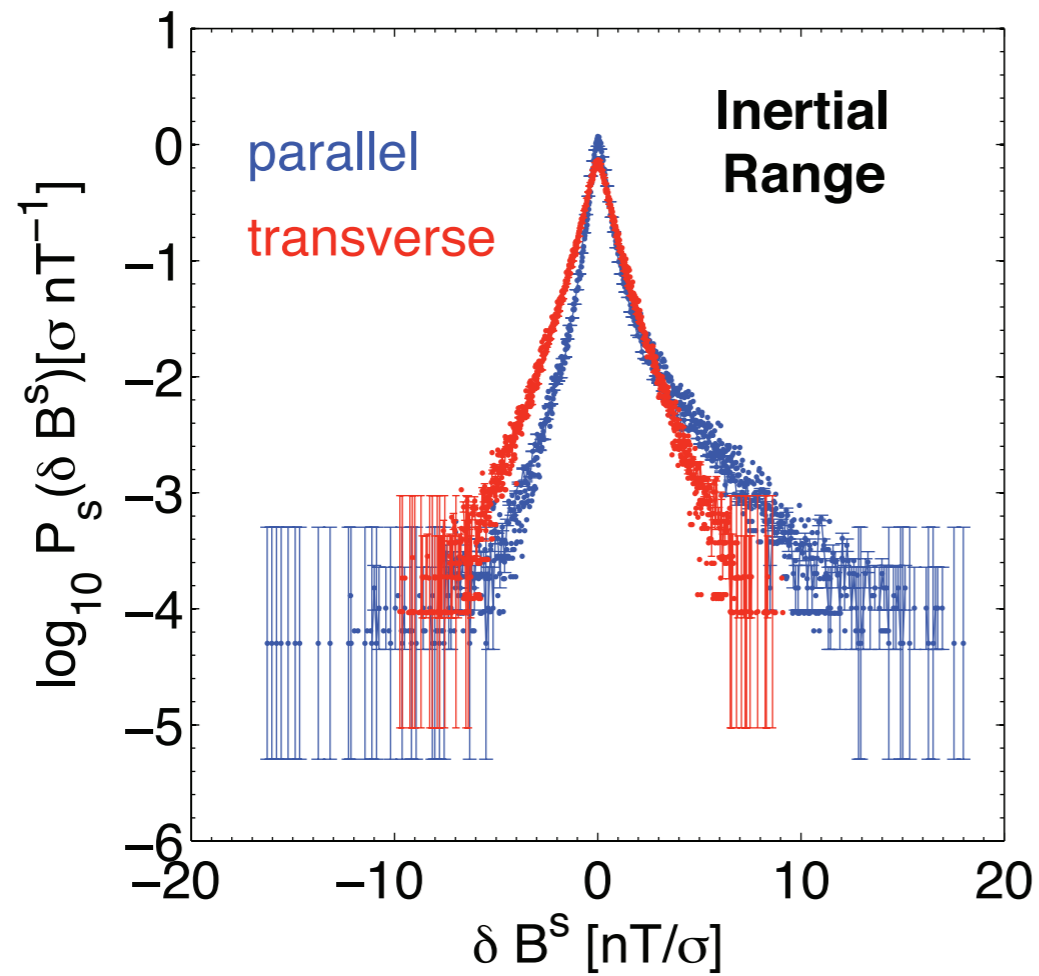
Structure Functions

$$S_{\parallel(\perp)}^m(\tau) = \frac{1}{N} \sum_{j=1}^N \left| \frac{\delta B_{\parallel(\perp)}(t_j, \tau)}{\sqrt{\tau}} \right|^m$$

note: Inertial range data is from ACE

Also see:
K. H. Kiyani et al.
Phys. Rev. Lett.
103, 075006 (2009)

standardised probability densities



isotropy

Kiyani et al.
ApJ (2013)

Effects of varying plasma beta [ERMHD]

$$\frac{\partial \mathbf{B}_\perp}{\partial t} = -\frac{c}{4\pi en_e} \nabla_\perp \times [\mathbf{B} \cdot \nabla \mathbf{B}_\parallel]$$

$$\frac{\partial \mathbf{B}_\parallel}{\partial t} = -\frac{\beta_i (1 + Z/\tau)}{2 + \beta_i (1 + Z/\tau)} \frac{c}{4\pi en_e} \nabla_\perp \times [\mathbf{B} \cdot \nabla \mathbf{B}_\perp]$$

includes density variations in a linear way
Schekochihin (2009) and Cho & Lazarian (2009)

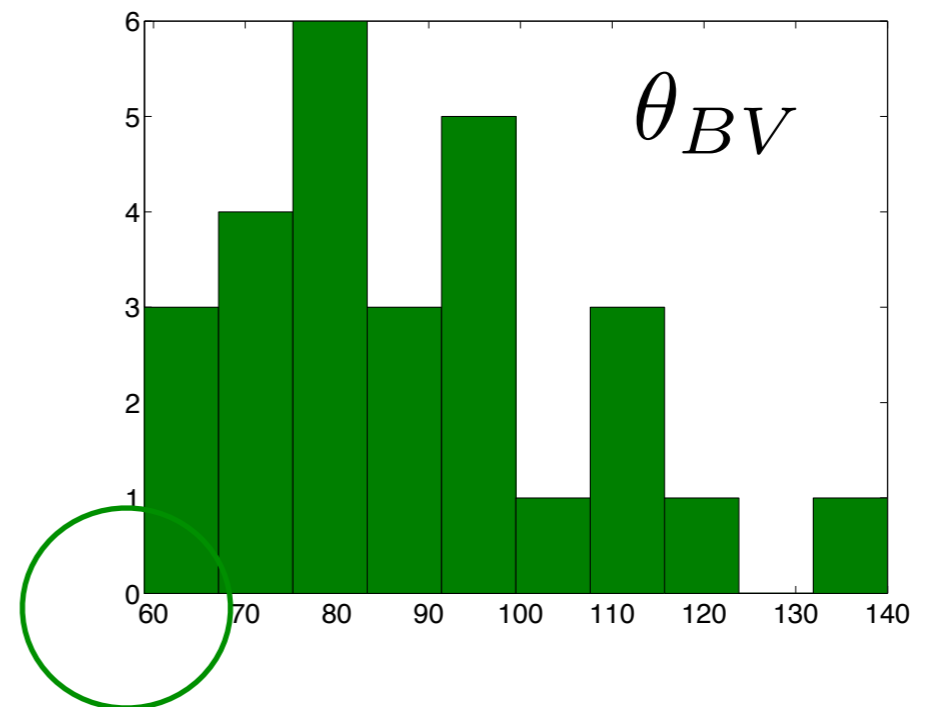
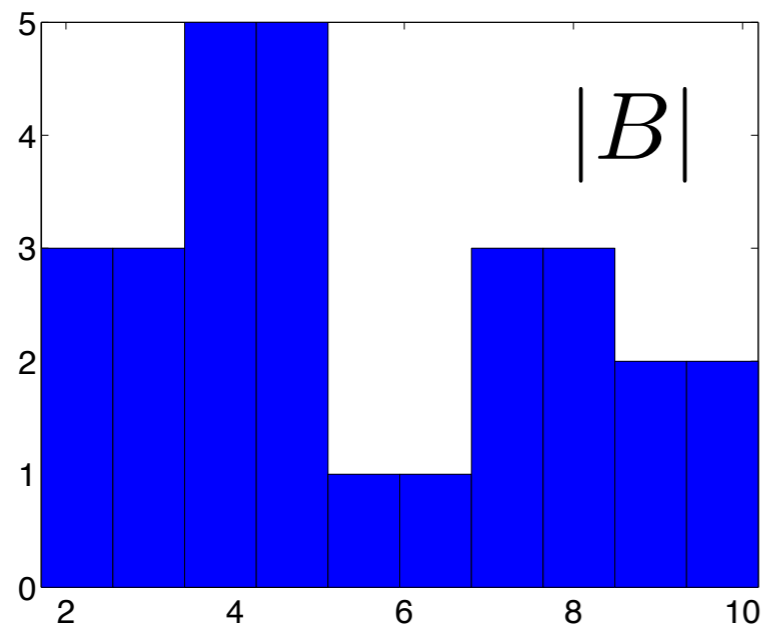
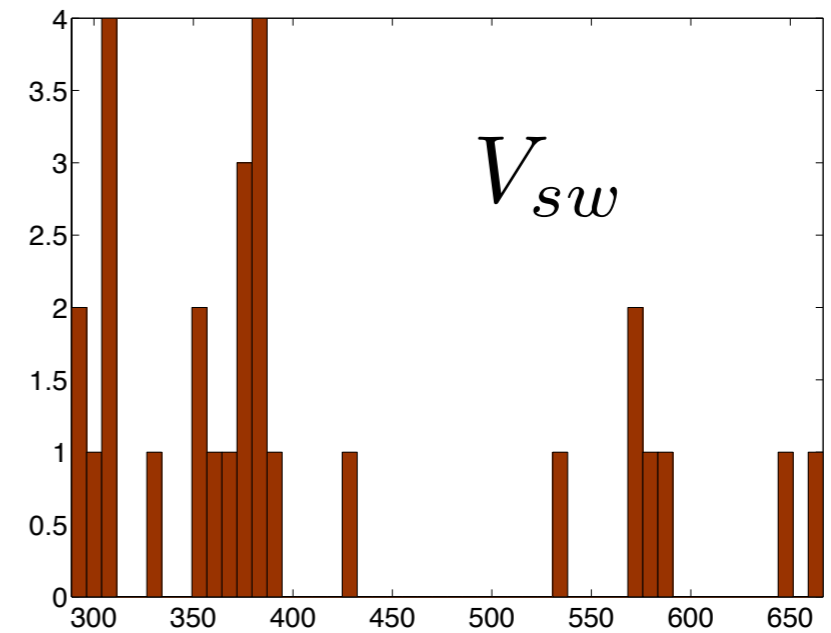
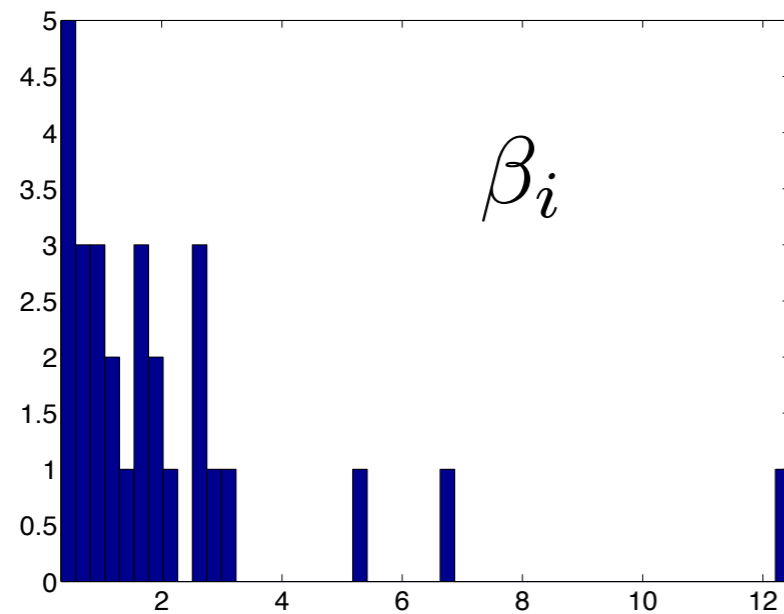
Survey study

Interval	Date/Time (UT)	SC	B [nT]	$\sigma_{ B }$	β_i	σ_{β_i}	n_i [cm ⁻³]	σ_{n_i}	T_e/T_i	σ_{T_e/T_i}	$T_{i\parallel}/T_{i\perp}$	$\sigma_{T_{i\parallel}/T_{i\perp}}$	V _{sw} [km s ⁻¹]	$\sigma_{V_{sw}}$	θ_{BV} [deg]	$\sigma_{\theta_{BV}}$	Sample Size
01	2006/03/07 14:00-14:32 UT	[3,3,2]	3.01	12.35	3.17	46.67	6.42	4.87	2.17	28.82	1.16	46.31	384.32	0.78	79.00	18.99	43,905
02	2006/03/07 14:32-14:53 UT	[3,3,2]	2.42	9.81	5.21	33.27	6.79	4.18	2.15	30.02	1.08	40.23	382.15	0.81	92.00	15.22	31,499
03	2006/03/07 14:53-15:04 UT	[3,3,2]	1.71	28.46	12.45	75.86	6.89	4.23	2.34	31.53	1.05	44.19	380.00	0.71	82.00	25.61	16,498
04	2006/03/07 15:04-15:40 UT	[2,3,2]	3.06	10.27	2.89	39.32	6.74	5.38	2.37	26.04	1.07	42.45	376.95	3.01	96.00	10.42	49,906
05	2007/01/27 18:00-19:50 UT	[3,1,2]	4.84	2.36	1.08	31.86	11.96	5.17	2.71	30.81	1.29	46.65	301.65	1.81	140.00	10.00	151,406
06	2007/01/27 21:20-21:50 UT	[3,3,2]	4.34	4.33	2.00	29.68	15.41	3.64	2.22	28.35	1.10	44.52	309.75	0.65	86.00	5.81	40,905
07	2007/01/27 21:50-23:20 UT	[3,3,2]	4.78	5.25	1.63	28.04	15.25	3.88	2.21	24.99	1.04	38.97	309.42	0.83	99.00	9.09	130,906
08	2004/02/22 03:10-04:20 UT	[3,3,2]	8.75	2.32	0.57	26.78	12.39	3.84	2.76	25.75	1.28	47.11	383.45	1.90	73.00	10.96	100,905
09	2004/02/22 04:20-04:50 UT	[3,3,2]	8.18	2.80	0.74	25.65	12.89	5.06	2.50	22.34	1.32	43.51	374.27	1.55	87.00	11.49	40,906
10	2004/02/24 17:10-18:10 UT	[3,1,NA]	5.57	1.40	0.93	45.45	7.64	4.36	NA	NA	0.91	62.11	388.67	1.57	71.00	14.08	81,810
11	2004/02/21 17:24-17:50 UT	[3,3,2]	8.49	2.06	0.43	25.15	9.12	3.81	2.98	23.02	1.46	35.89	376.24	0.73	66.00	7.58	38,999
12	2004/02/21 18:15-19:30 UT	[3,3,2]	8.45	4.02	0.49	30.06	9.69	7.50	2.78	24.26	1.31	45.16	368.87	1.46	85.00	15.29	108,406
13	2007/02/05 15:40-19:10 UT	[3,3,1]	4.93	5.46	1.00	22.71	8.49	4.47	2.53	14.63	1.08	24.05	331.67	0.92	97.00	8.25	306,812
14	2007/02/22 12:10-13:30 UT	[4,3,1]	3.24	5.75	1.84	29.23	11.41	8.11	3.37	19.00	1.00	35.23	304.50	3.79	110.00	12.73	108,518
15	2007/02/22 13:30-14:20 UT	[4,3,1]	2.23	29.42	6.68	51.40	12.88	10.37	2.59	15.95	0.82	28.55	305.62	2.39	111.00	8.11	74,999
16	2007/02/22 14:20-17:00 UT	[4,3,1]	4.14	5.81	1.11	25.56	9.15	9.48	2.65	15.46	0.93	26.45	296.07	4.50	109.00	5.50	235,907
17	2004/01/27 00:00-02:00 UT	[3,1,1]	9.87	3.84	0.44	14.32	7.87	7.96	1.82	12.38	0.81	20.58	428.90	1.40	102.00	6.86	171,812
18	2007/02/23 01:50-02:50 UT	[1,1,1]	3.62	3.06	1.65	21.73	9.01	2.94	2.68	17.64	0.84	27.93	288.81	0.67	NaN	NaN	81,812
19	2007/01/30 05:20-08:10 UT	[1,1,2]	6.01	4.98	1.54	44.87	2.75	7.95	0.41	43.48	0.67	61.00	649.29	2.75	77.00	20.78	246,818
20	2002/02/19 00:32-01:10 UT	[3,1,2]	9.18	8.43	0.94	46.14	27.97	7.76	1.53	46.24	1.18	67.59	353.42	0.98	116.00	6.90	56,999
21	2002/02/19 01:10-02:45 UT	[3,1,2]	7.45	11.31	1.64	47.89	27.79	11.58	1.46	42.18	0.90	55.03	364.10	1.00	80.00	23.75	142,500
22	2002/02/19 02:45-03:30 UT	[3,1,2]	10.18	2.66	0.33	34.57	13.40	7.00	3.30	32.71	0.85	52.45	356.48	1.98	70.00	11.43	63,405
23	2001/04/05 22:35-23:32 UT	[1,1,2]	7.29	5.29	0.75	36.91	3.10	18.63	0.85	42.45	0.53	52.84	533.51	1.69	95.00	7.37	67,027
24	2002/02/11 19:19-20:29 UT	[3,1,2]	7.45	2.52	0.77	36.32	3.55	6.40	1.23	32.90	0.91	49.12	569.55	2.33	82.00	13.41	96,812
25	2007/01/30 00:00-01:20 UT	[4,1,4]	4.52	7.30	2.58	51.48	2.57	6.90	0.45	41.92	0.75	58.89	666.52	2.35	75.00	24.00	2,151,828
26	2007/01/20 12:10-13:20 UT	[3,1,4]	3.83	3.33	2.10	53.64	1.75	9.06	0.44	51.58	0.54	59.57	588.85	2.43	78.00	14.10	1,890,002
27	2007/01/20 13:20-14:10 UT	[3,1,4]	3.45	3.71	2.54	67.42	1.88	7.28	0.56	70.28	1.16	57.71	577.89	3.03	59.00	21.53	1,350,005
28	2007/03/28 04:00-04:40 UT	[4,1,4]	4.06	4.44	2.68	54.38	2.32	6.56	0.49	57.37	0.86	55.87	568.74	2.79	66.00	22.73	1,071,818

Table A1

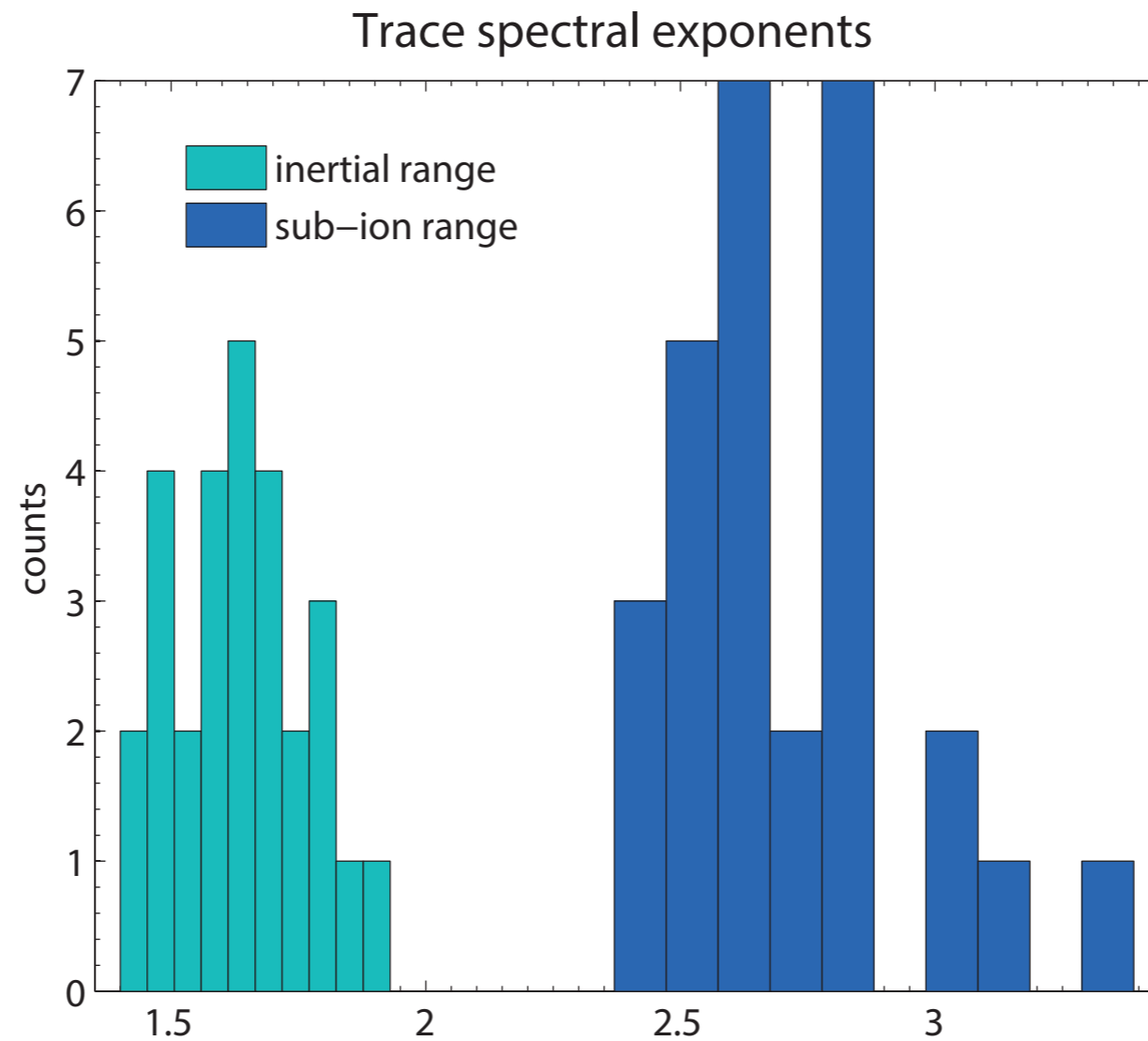
Plasma parameters, along with their variability/errors for all 28 Cluster intervals used in this study: SC is the particular Cluster spacecraft used for the [FGM/STAFF-SC,CIS,PEACE] instrument respectively in the interval; |B| is the magnetic field magnitude; β_i , n_i and V_{sw} are the ion plasma beta, number density and solar wind speed respectively; T_e and T_i are the electron and ion temperatures respectively; θ_{BV} is the angle between the local background magnetic field and the mean solar wind velocity vectors; and \parallel and \perp designate parallel and perpendicular to the magnetic field vector respectively. All these quantities are mean averages over the interval. All 'errors' (labelled with σ) are percentage errors, calculated by dividing the typical variability – represented by the standard deviation – of the relevant quantity in the interval by the mean value. Intervals 25-28 are intervals where the instruments were operating in burst mode i.e. where the magnetic field sampling (after joining the FGM and STAFF-SC signals) is approximately 450 Hz; the rest of the intervals are sampled in normal mode with nominal magnetic field sampling at approximately 25 Hz.

28 data intervals from the cluster mission



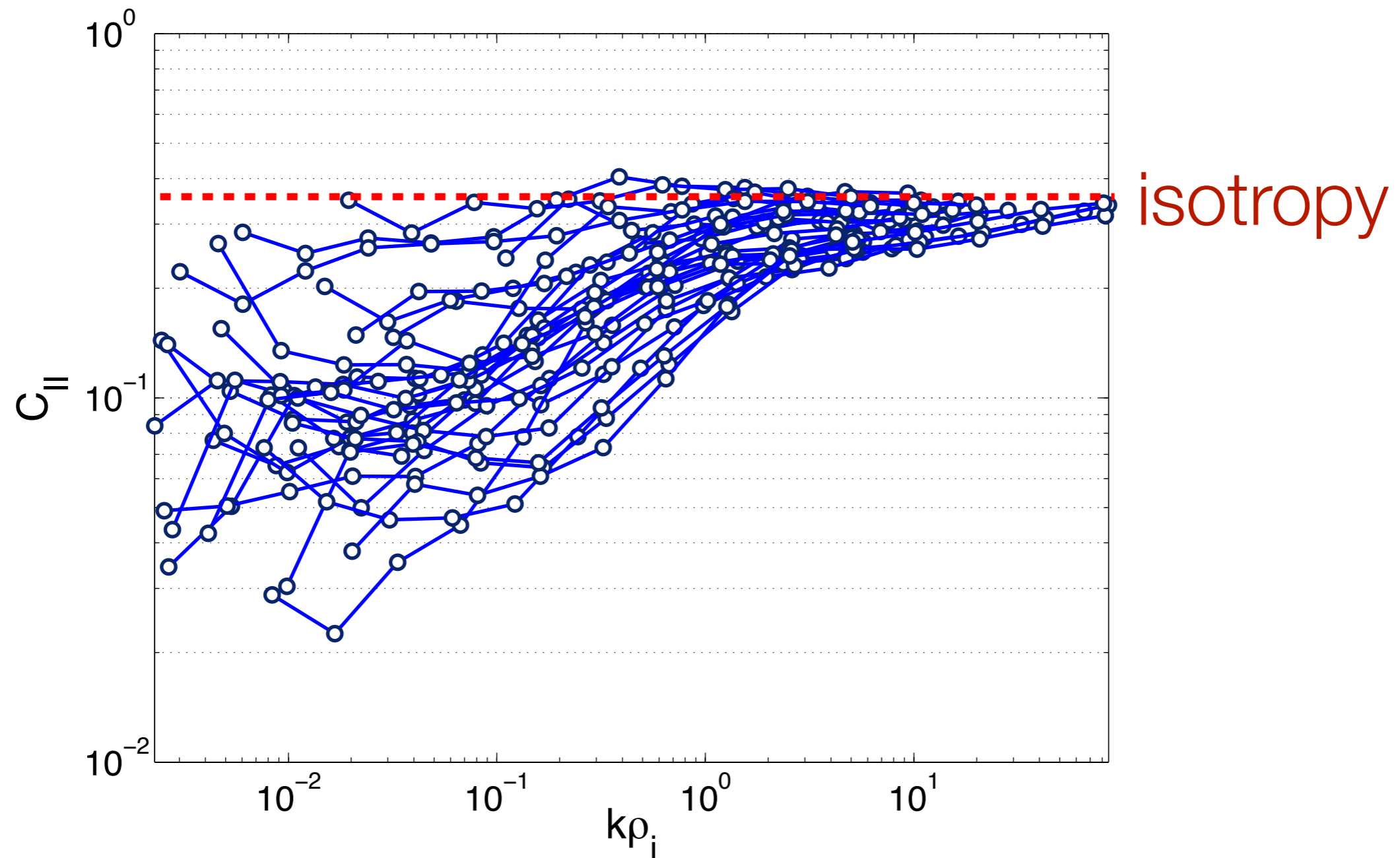
stationary plasma parameters

results: spectral slopes (trace)



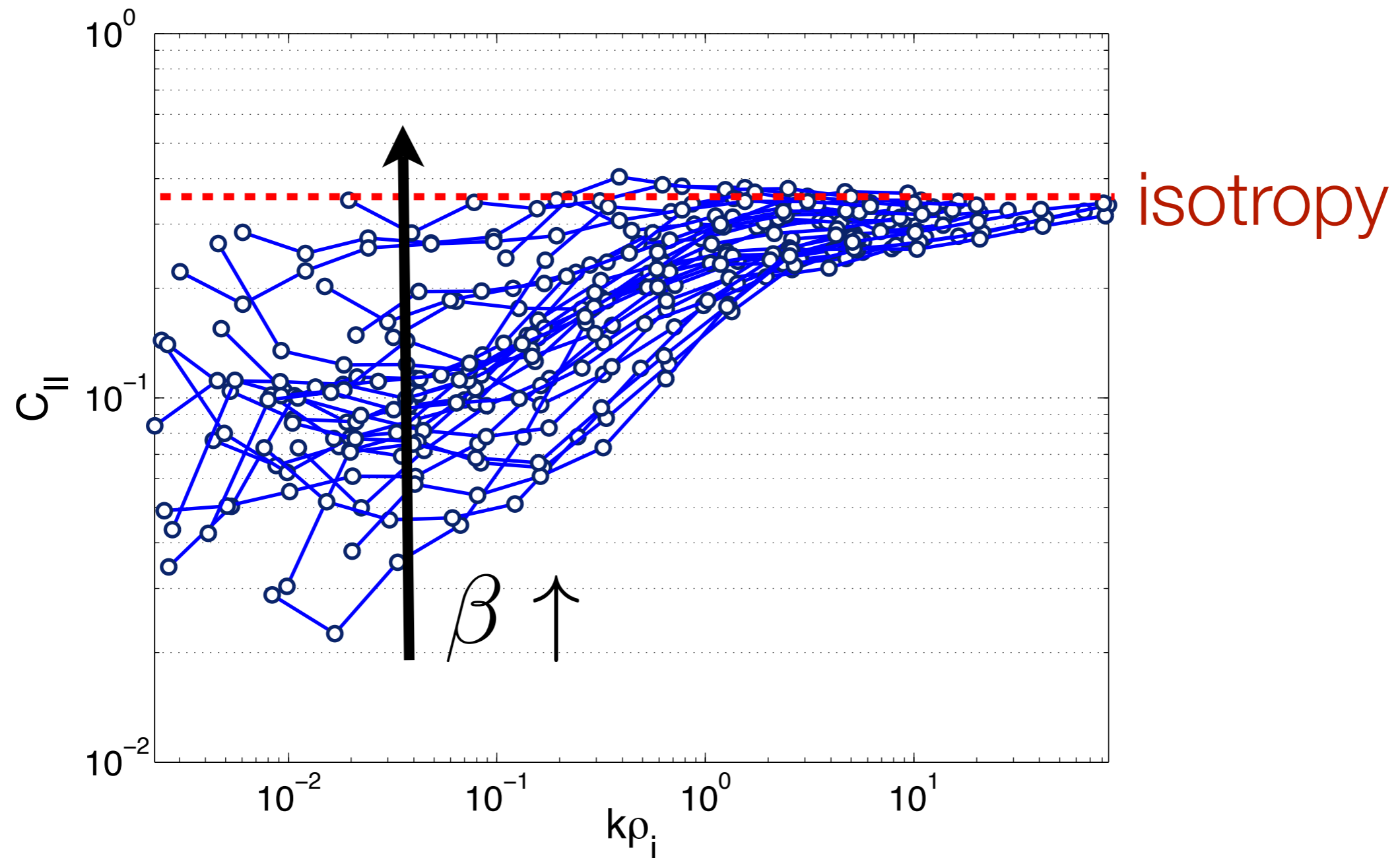
see also: Smith et al. (2006) and Sahraoui et al. (2013)

Magnetic compressibility variation with beta



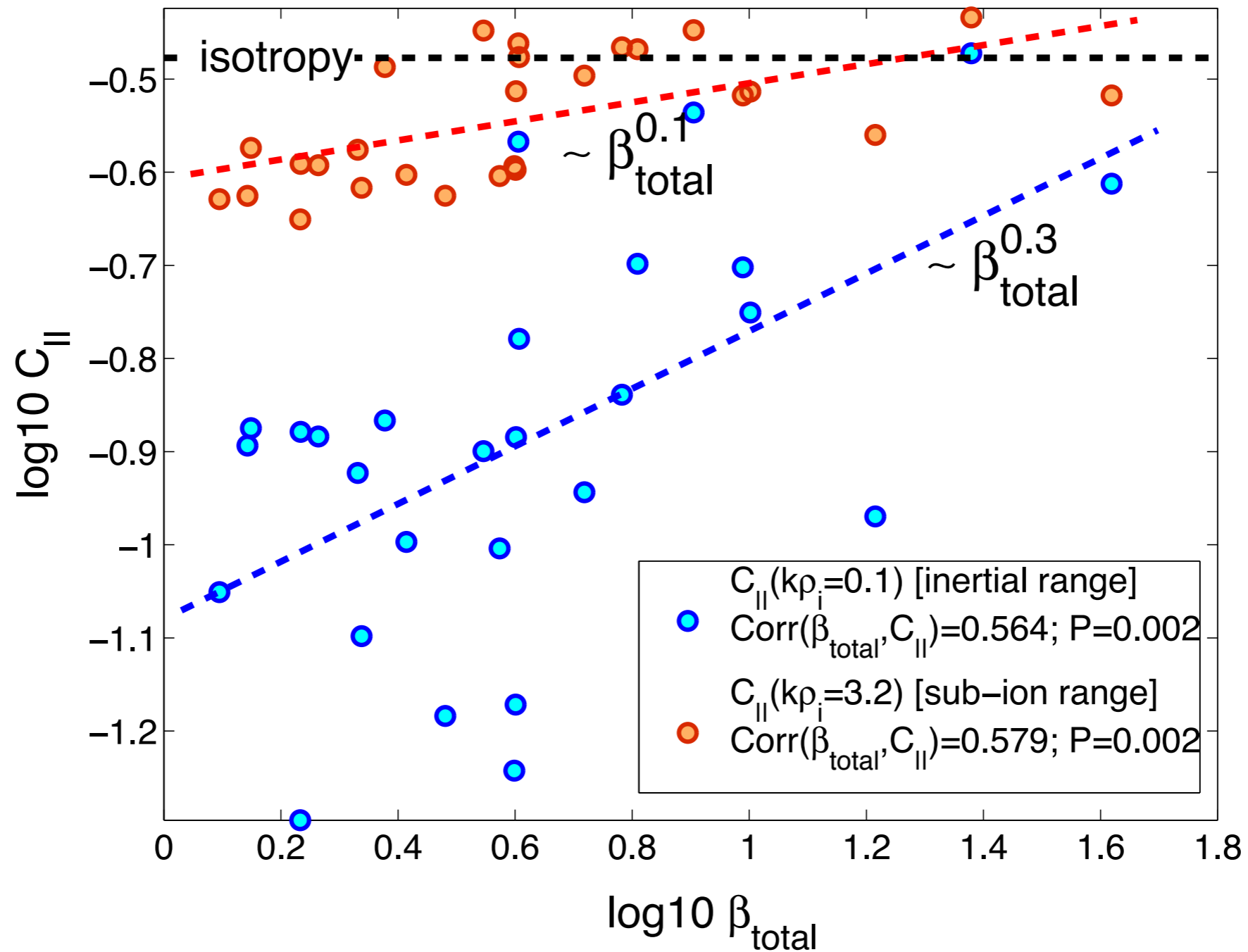
see also:
Smith, Vasquez and
Hamilton, JGR (2006)

Magnetic compressibility variation with beta



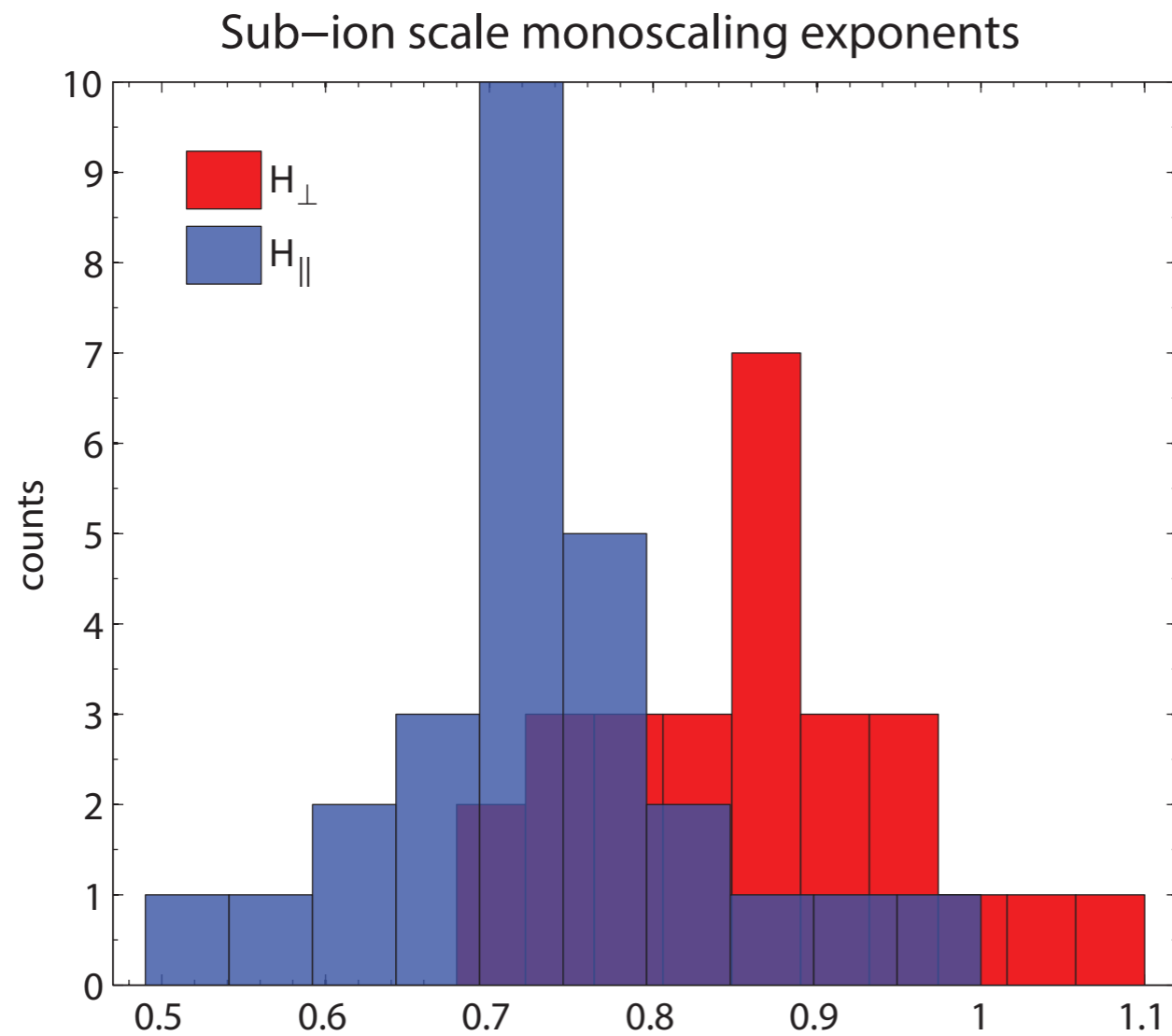
see also:
Smith, Vasquez and
Hamilton, JGR (2006)

Magnetic compressibility variation with beta



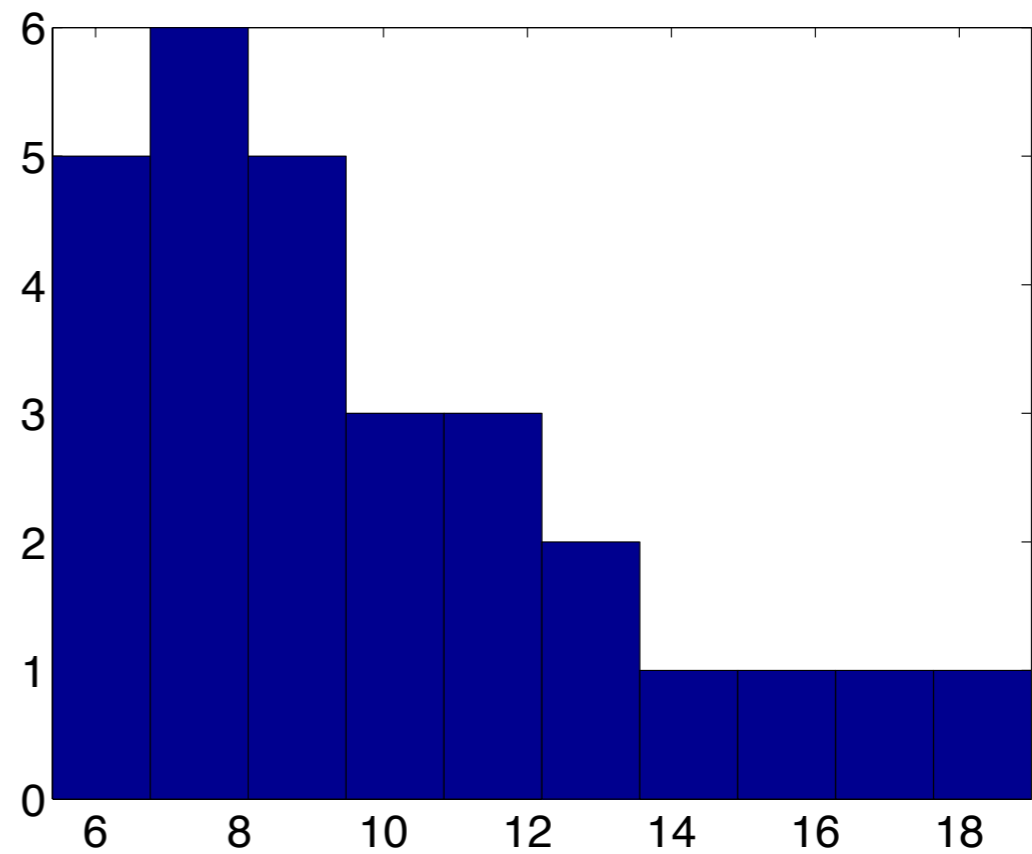
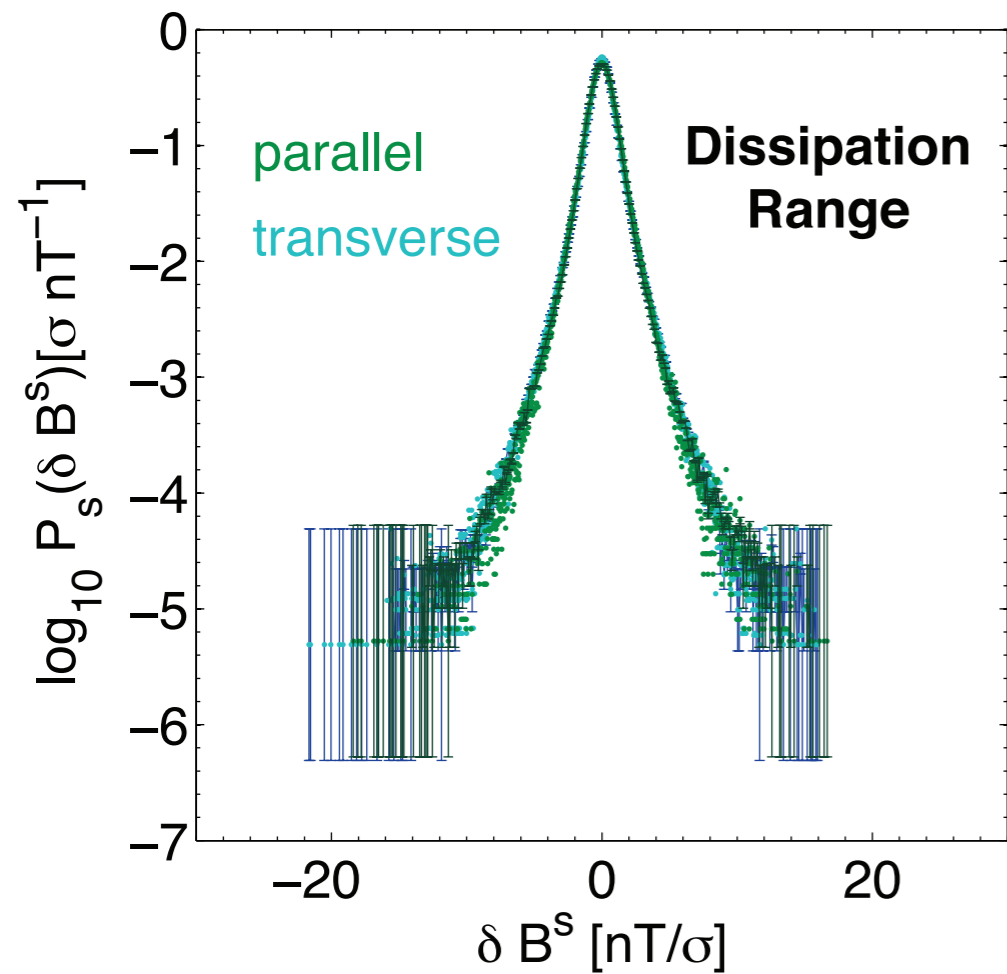
results: scaling

all monoscaling at sub-ion scales



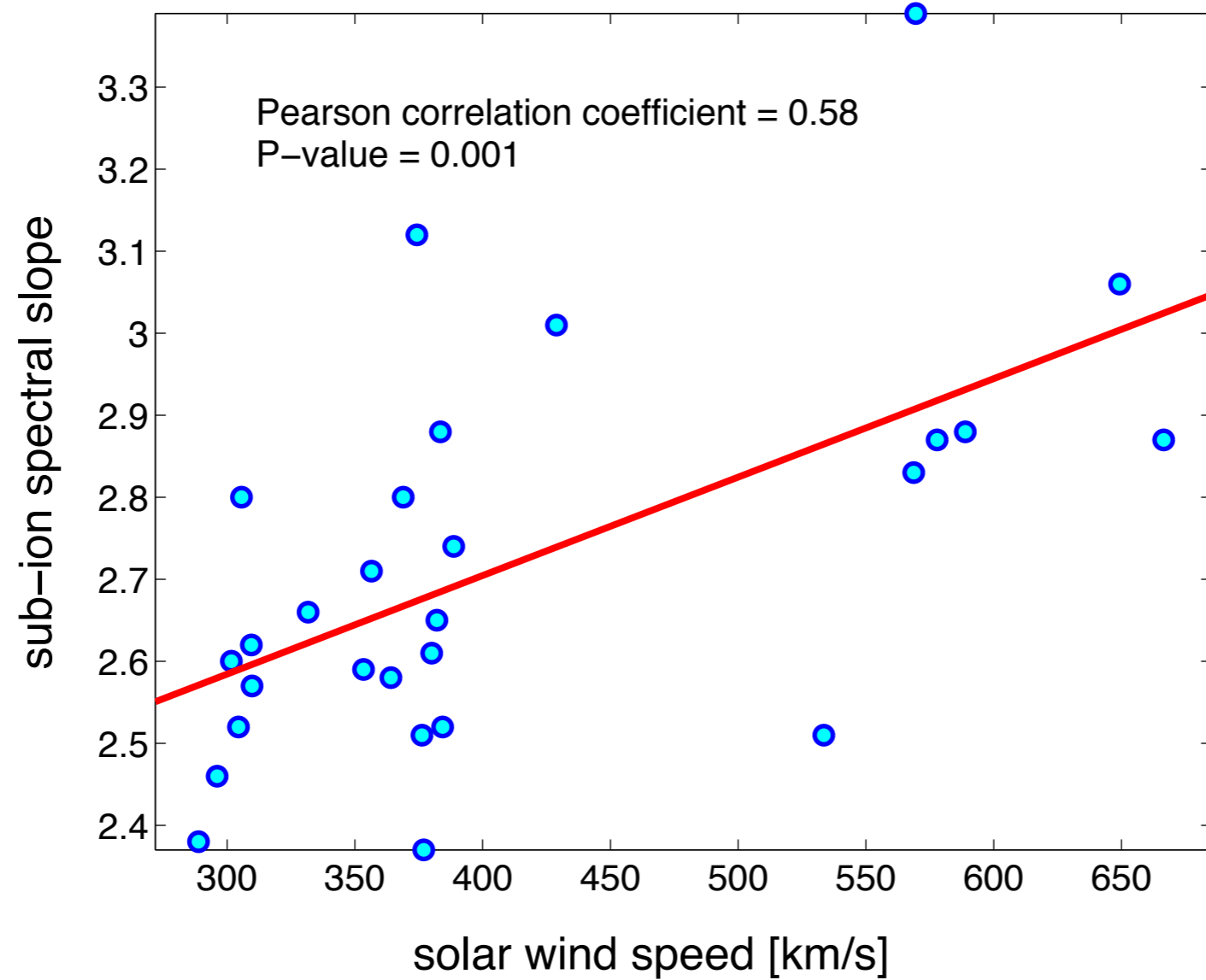
$$H_{\perp} > H_{\parallel}$$

results: intermittency and heavy tails

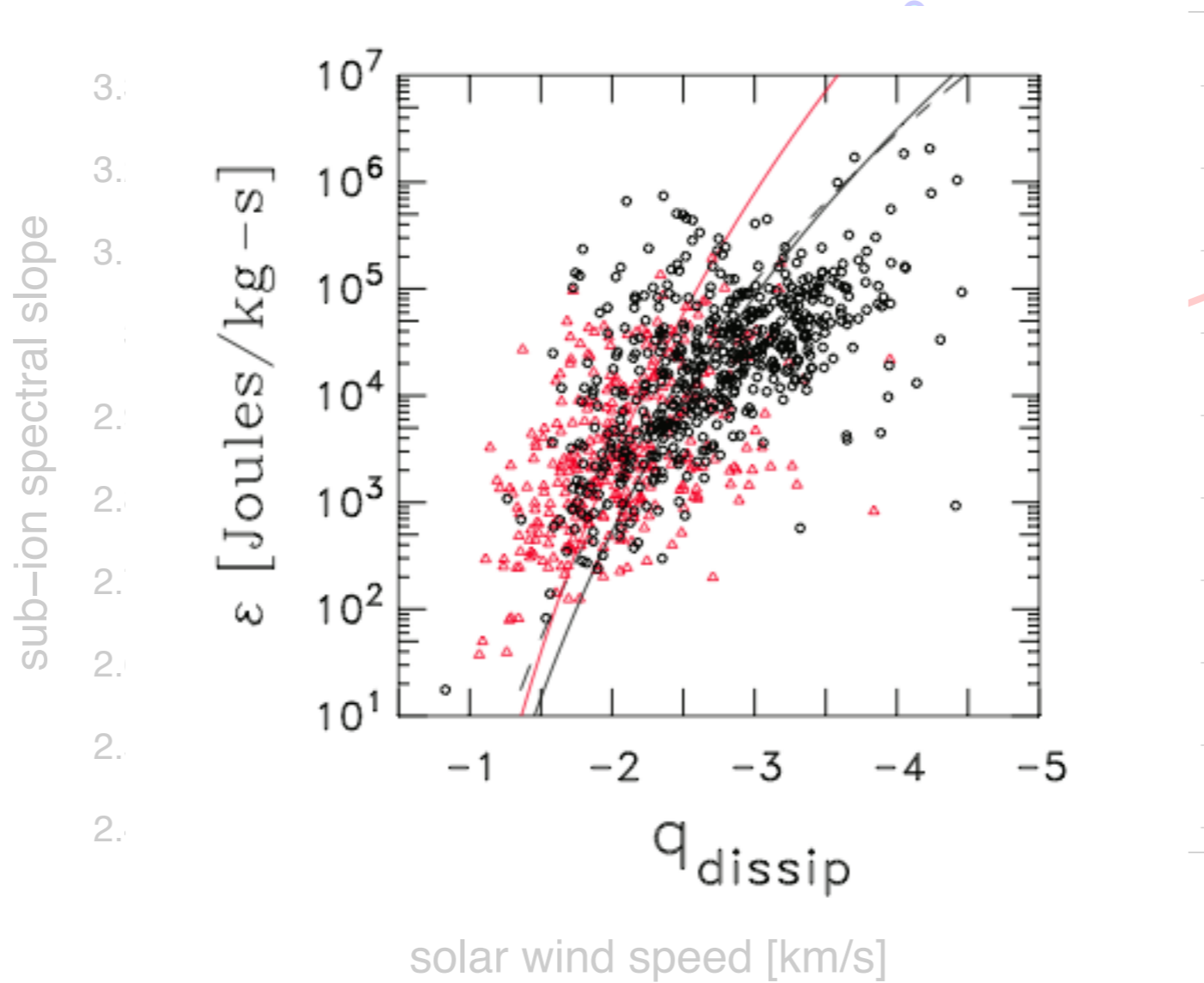


kurtosis

results: solar wind speed variation



results: solar wind speed variation



Macbride, Smith & Foreman (2008) and
Smith et al. (2006)

Scaling, fractals and physics

Monofractal dissipation

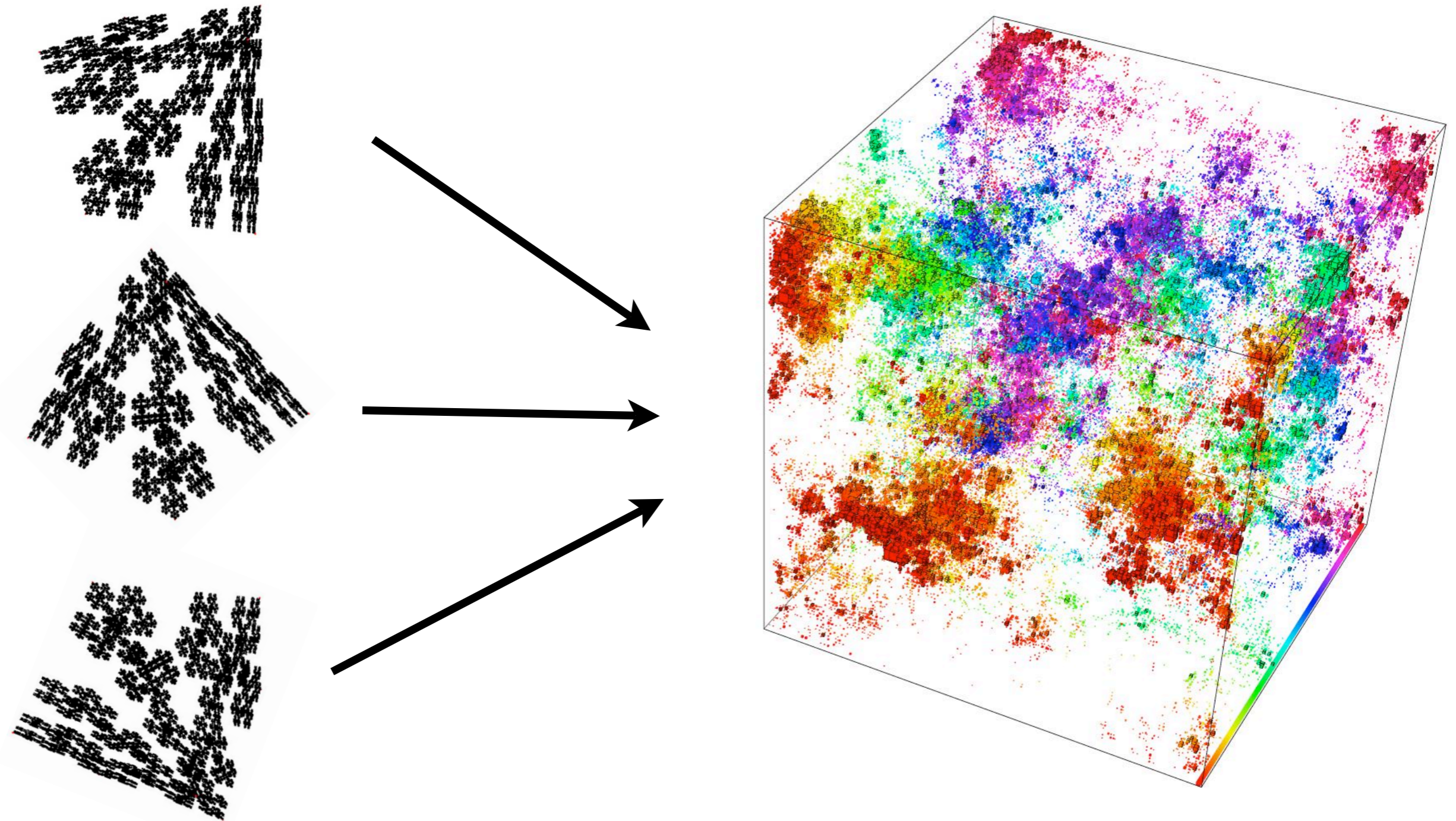


Single exponent H
living on a fractal set of
dimension D where
dissipation occurs

Global Scale Invariance

Cantor 'dust' courtesy of Andrew Top: <http://www.andrewtop.com/IFS3d/IFS3d.html>

Multifractal dissipation

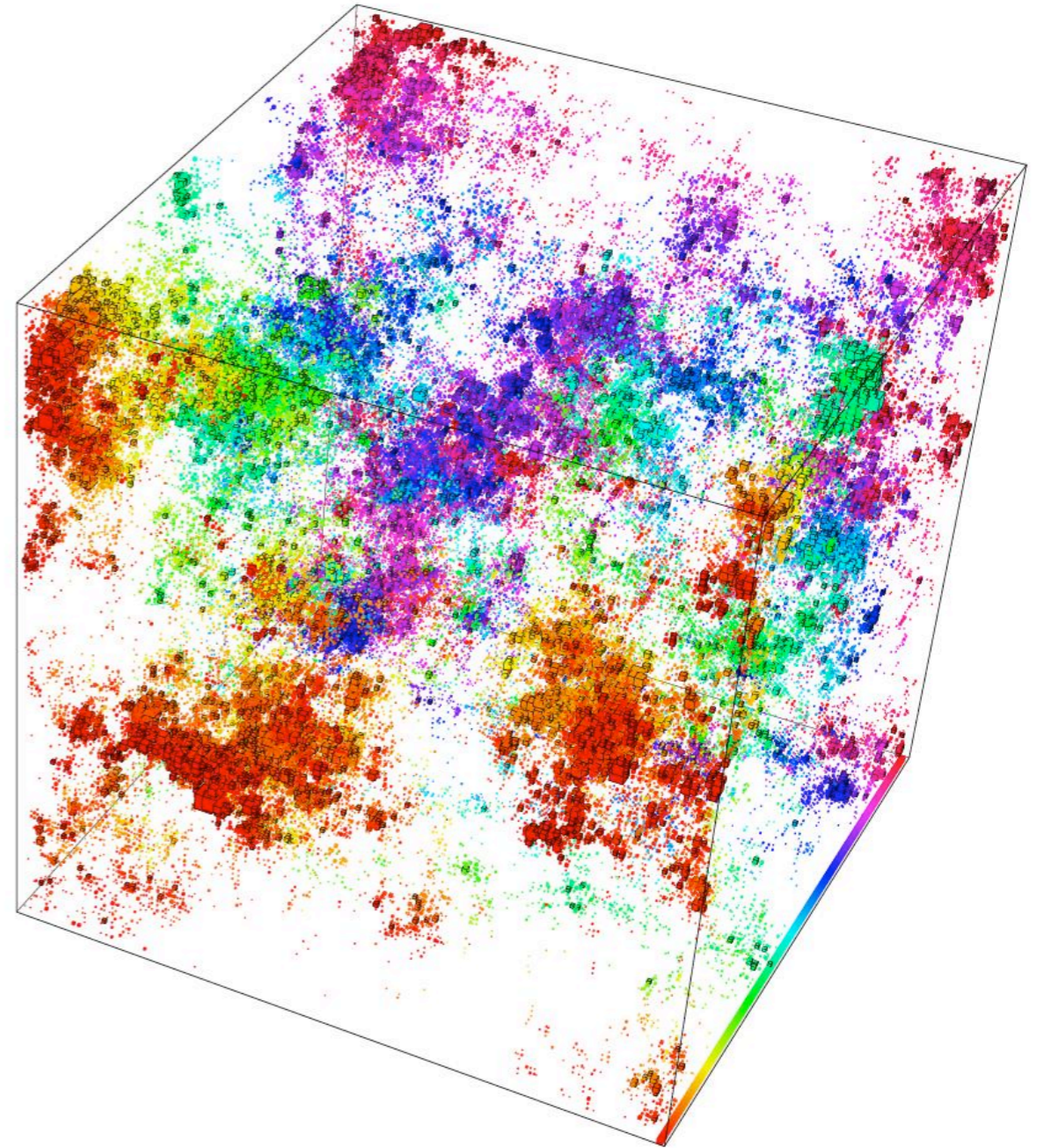


Courtesy of R. Roemer (Warwick): multifractal electronic wavefunction at metal insulator transition in 3D Anderson model

Multifractal dissipation

multiple exponents h
living on a fractal sets of
dimension $D(h)$ where
dissipation occurs

Local Scale Invariance



Speculation on the physics

EUROPHYSICS LETTERS

1 March 1991

Europhys. Lett., 14 (5), pp. 439-444 (1991)

A Prediction of the Multifractal Model: the Intermediate Dissipation Range.

U. FRISCH(*) and M. VERGASSOLA(*)(**)

(*) *CNRS, Observatoire de Nice - B.P. 139, 06003 Nice Cedex, France*

(**) *Dipartimento di Fisica, Università «La Sapienza»*

P.le A. Moro 2, I-00185 Roma, Italy

(received 1 November 1990; accepted in final form 12 December 1990)

PACS. 47.25C – Isotropic turbulence.

Abstract. – It is shown that the multifractal model of fully developed turbulence predicts a new form of universality for the energy spectrum $E(k)$, which can be tested experimentally. Denoting by R the Reynolds number, $\log E/\log R$ should be a universal function of $\log k/\log R$. This includes an *intermediate dissipation range* in which a continuous range of multifractal scaling exponents are successively turned off by viscosity.

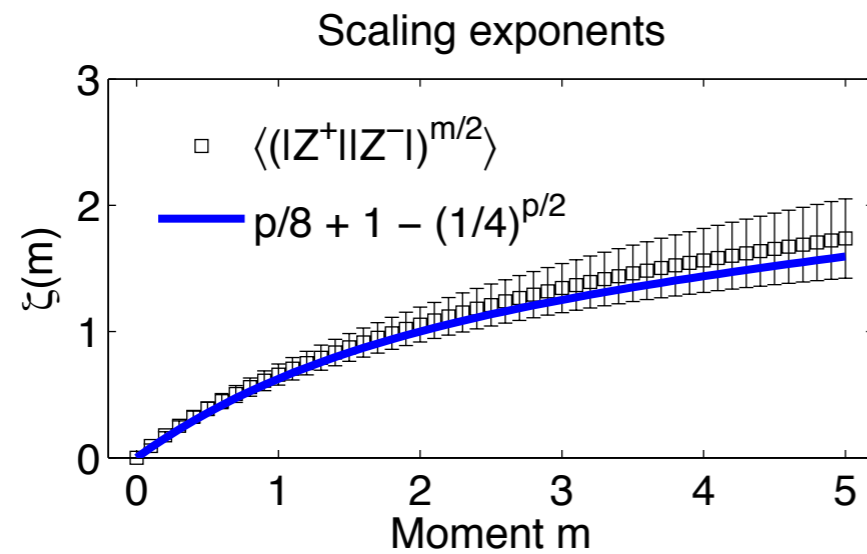
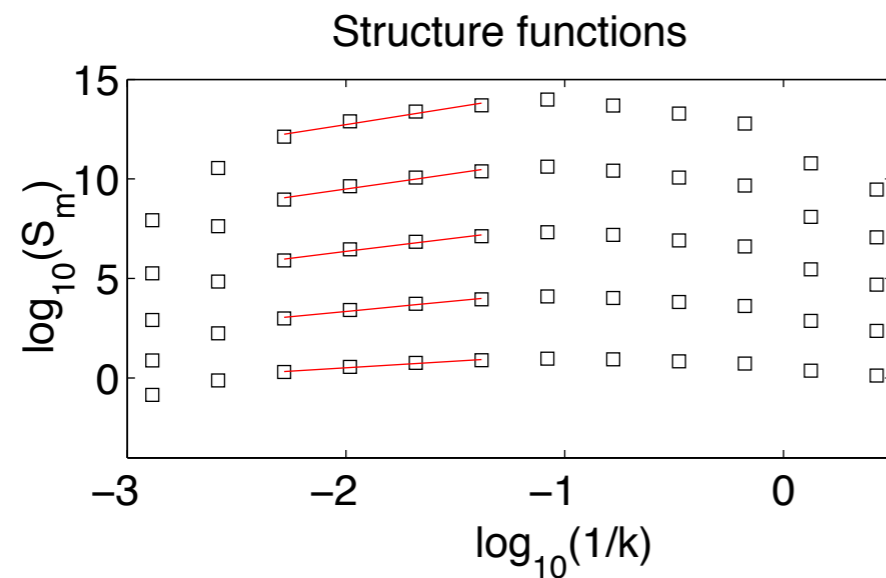
see also Chevillard, Castaing, and Levêque, *Eur. Phys. J. B* 45, 561–567 (2005)

Using fluid models to explore structural changes

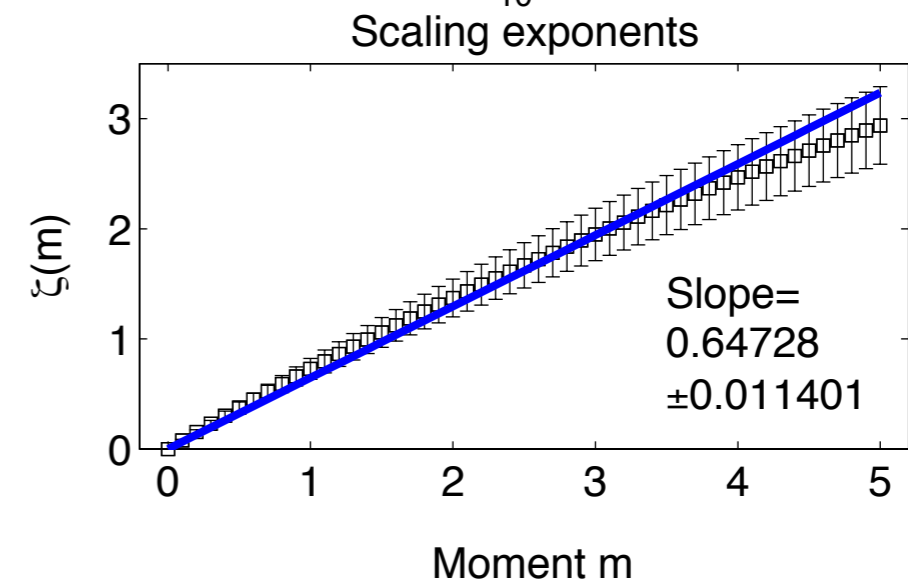
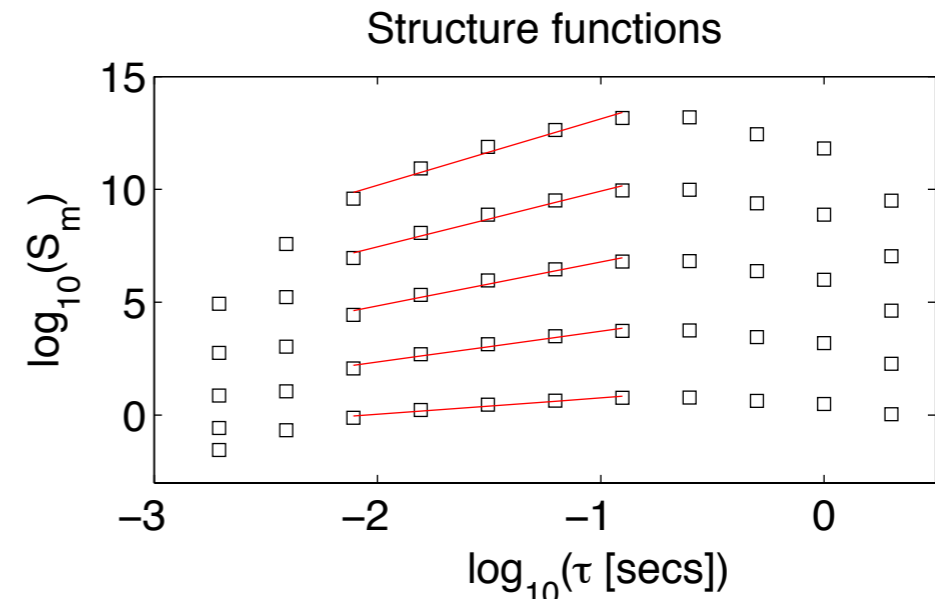
Use simulations to see if the scaling can be replicated by fluid models containing relevant physics and to explore the topology of structures involved

Using fluid models to explore structural changes

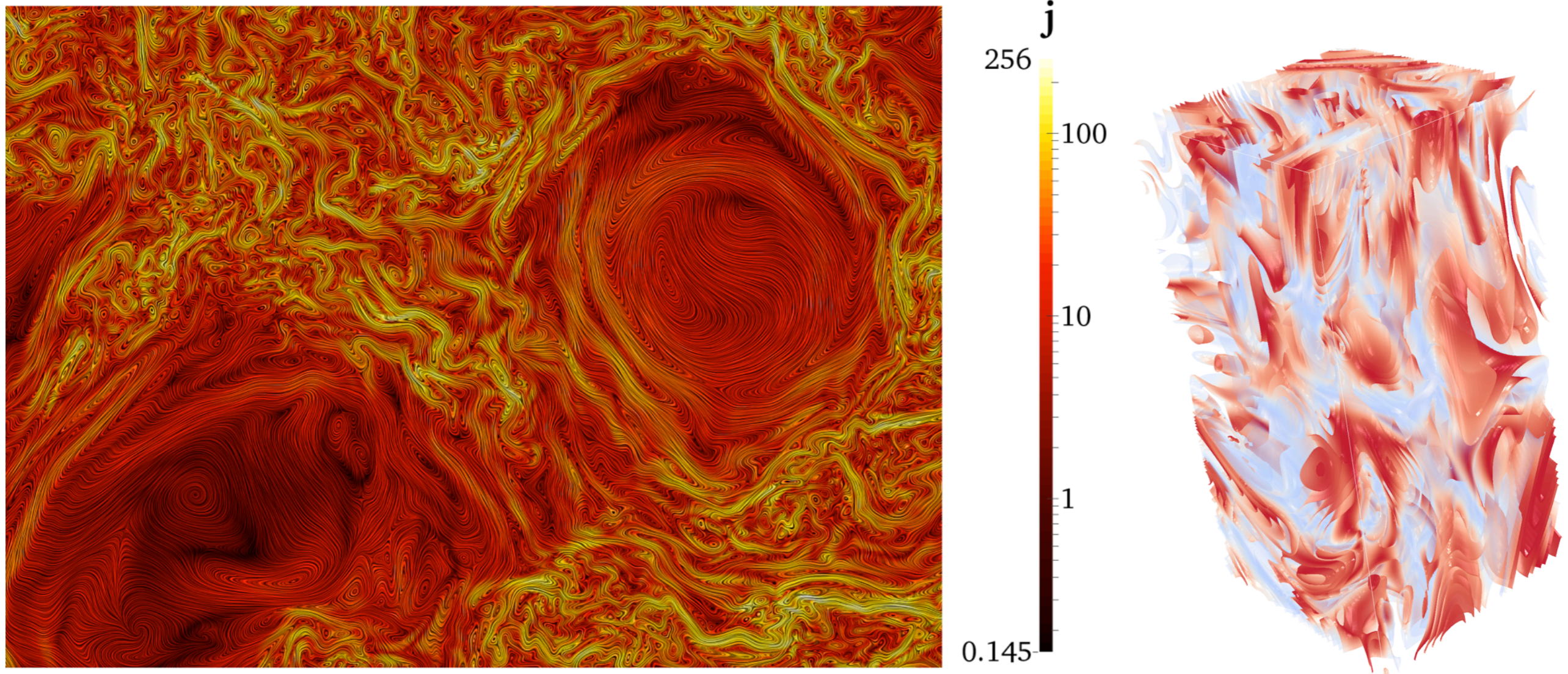
MHD



EMHD

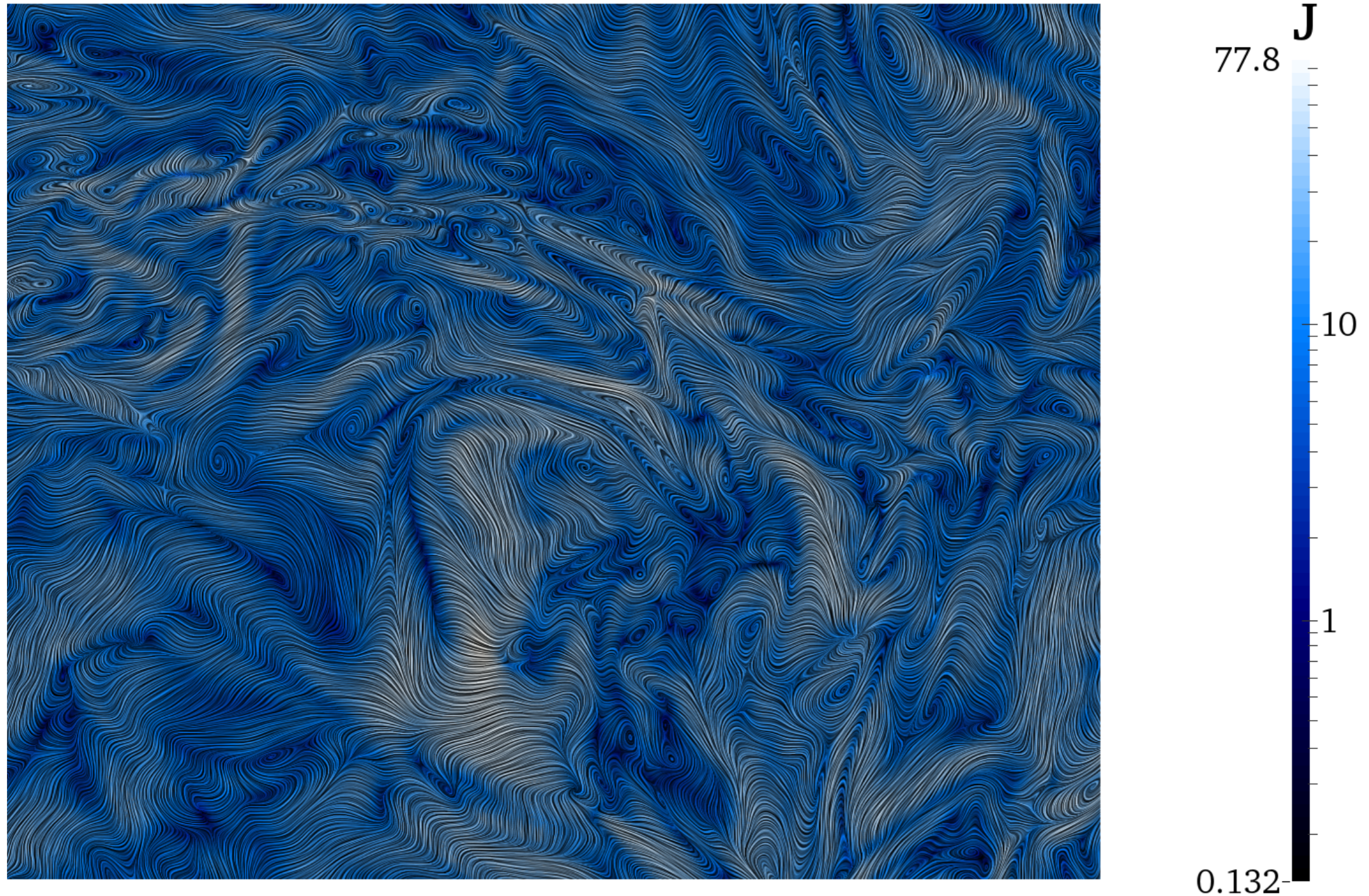


LIC visualisation -- mostly current sheets in MHD



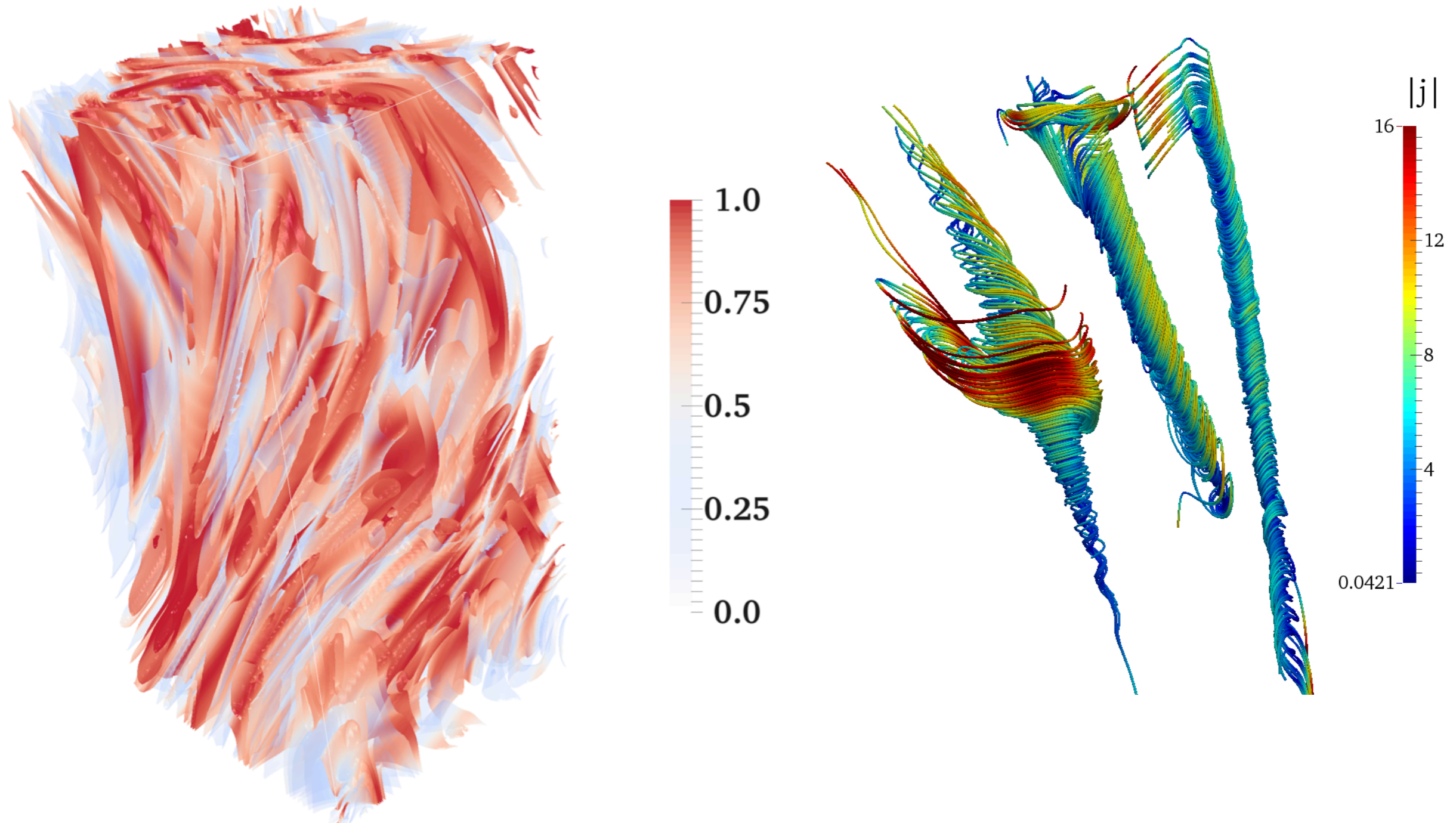
MHD with strong guide field [$1536^2 \times 128$ decaying]

LIC visualisation of filamentary structures in EMHD



Electron MHD [1024^3 decaying]

visualisation of filamentary structures in EMHD -- Beltrami fields $[(\text{Curl } \mathbf{B}) \times \mathbf{B}=0]$ & Hall physics



take home message

- Enhanced magnetic compressibility @ sub-ion scales. With strong beta variation.
- Near component isotropy at sub-ion scales.
- PDFs show higher levels of intermittency at such scales; ubiquitous multi->monoscaling transition [in all intervals.](#)
- Simulations reproduce this scaling behaviour and -- using them as a proxy for what is happening -- we see that there is a **transition from a current sheet dominated regime to one which is filament dominated.**